Galetto, F., Asfora, B. and Pritchard, M. E. (2026) “Evaluating steady-state volcanism in Iceland, La Réunion, Hawai‘i and western Galápagos: connections with volcanic hazards and future perspectives”, *Volcanica*, 9(1). doi: 10.30909/vol/kgch7634.

Evaluating steady-state volcanism in Iceland, La Réunion, Hawai‘i and western Galápagos: connections with volcanic hazards and future perspectives

Authors: Federico Galetto[1,2], Beatriz Asfora[3], Matthew E. Pritchard[1]*

[1]Cornell University; Earth and Atmospheric Sciences Department; Ithaca, NY, USA

[2] Now at Istituto Nazionale di Geofisica e Vulcanologia – Osservatorio Nazionale Terremoti; Roma, Italy.

[3] Cornell University; Sibley School of Mechanical and Aerospace Engineering; Ithaca, NY, USA

** Corresponding Author: Federico Galetto (federico.galetto@ingv.it)*

ORCiD (FG): 0000-0001-9469-3968

ORCiD (BA): 0000-0003-3726-2947

ORCiD (MEP): 0000-0003-3616-3373

Abstract

Steady state volcanoes and magmatic provinces erupt magmas at nearly constant rates over the decades. Here, we analysed the reliability of steady state volcanism and its relationship with volcanic hazard evaluation in terms of forecasting the erupted volume in four frequently erupting oceanic hot spots: Iceland, La Réunion, Hawai‘i and western Galápagos. Over decadal time spans, these hot spots show steady state activity often characterized by shorter-term cycles with an initial decrease in erupting rates, followed by an increase that rebalances the erupted volumes with the expected ones, providing a rough estimation of the maximum expected erupted volume of these paroxysmal periods. Although rarer, we also observe the opposite behaviour, with the eruption of more magma than expected, followed by low-rate periods proportional to the excess erupted volume. Steady-state rates can change over time, and future studies should investigate if these changes are related to longer-term episodes.

1) Introduction

G. Wadge introduced the concept of steady state volcanism at the beginnings of the 1980s for volcanoes that erupted magma at constant average rates over many years (Wadge, 1980, 1982; Wadge

29 & Guest, 1981). The steady state activity of a volcano can therefore be identified by constructing the
30 curve of cumulative volumes of erupted magma over time (Wadge, 1982). Figure 1 shows the
31 different types of behaviour observed in steady state volcanoes, as reported by Wadge (1982). The
32 type I (Figure 1) is characterized by continuous eruption rates matching with the steady state rates.
33 More often, steady state volcanism shows fluctuations in the activity, which can be divided in three
34 types (II-IV; Figure 1; Wadge, 1982). In type II, a series of eruptions with intervening repose periods
35 generate a step-shaped curve, where a characteristic volume range defines the limits of the maximum
36 erupted volumes and repose periods in this stage. Graphically, these limits are represented by two
37 lines parallel to the average steady state rate that envelope the step-shaped curve (Figure 1). Eruptions
38 with volume significantly higher than that expected by the steady state rates can be either followed
39 (type III; Figure 1) or preceded (type IV; Figure 1) by repose periods (or periods with very low
40 eruptive rates), whose duration is proportional to the volume erupted by these eruptions in order to
41 rebalancing the real erupted volumes with those expected by the steady state rates. Furthermore,
42 Wadge (1982) reported that the steady state activity can be interrupted by long-periods (also
43 centuries) of quiescence not followed by large volume eruptions, but from a resumption of the steady
44 state volcanism at the same or different rates. The opposite, which is a large volume eruption not
45 followed by a proportional period of quiescence but just by renewed activity at the previous steady
46 state rates, is rarer (Wadge, 1982). Thus, the activity of type III-IV shows a short-term (usually some
47 years) change in the eruptive rates that can mask the steady state characteristic of equilibrium between
48 the expected and the erupted volumes. However, by looking at the cumulative erupted volumes over
49 decades, it becomes evident how with the end of a type III or IV cycle the equilibrium between the
50 expected and the erupted volumes come back to be confirmed, supporting the steady state activity, as
51 observed in all volcanoes and magmatic provinces where steady state activity has been identified.

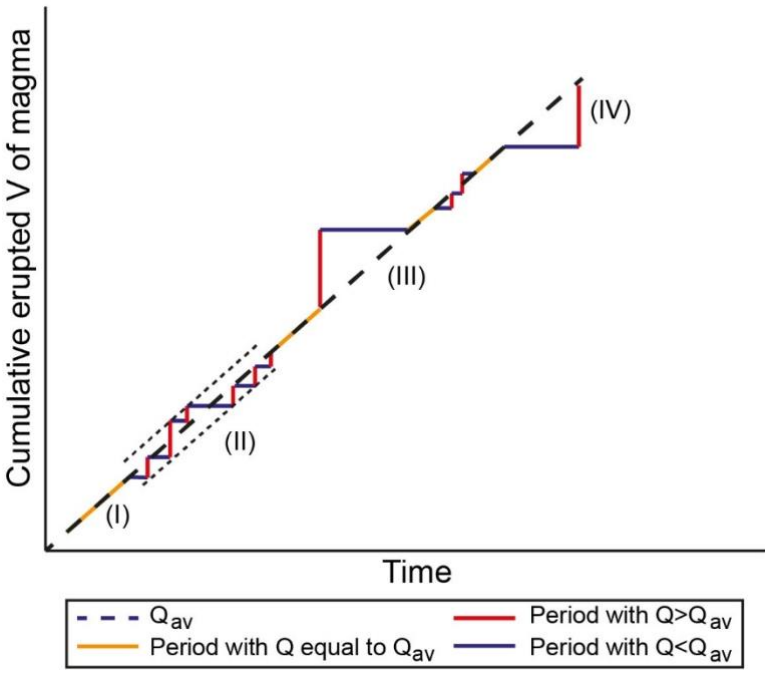

Figure 1. Schematic illustration of the main types (I-IV) of behaviour of the steady state activity (based on Wadge, 1982). For a detailed description of the types I-IV of behaviour see the beginning of the introduction. The black dashed line represents the average steady state rate (Q_{av}), while the orange, blue and red lines the cumulative volumes erupted over time (thus the observed eruptive rates Q). See Introduction for further details.

Different volcanoes have shown steady state activity, such as Mt. Etna (Italy), Piton de la Fournaise (La Réunion, France), Nyamuragira (Democratic Republic of Congo), Kīlauea (USA), Klyuchevskoy and Bezymianny (Russia), and Santiaguito (Guatemala) (e.g., Bonaccorso & Calvari, 2013; Coppola et al., 2021; Wadge, 1982). Ever since the theory of steady state volcanism was first proposed, it has been observed that steady state activity can be ascertained at different time scales (from decades to tens of kiloyears) and at both the scale of the single volcano and at the scale of the whole magmatic province (King, 1989; Kuntz et al., 1986; Lipman, 2000; Marturano et al., 2018; Singer et al., 1997, 2008; Wadge, 1982; Yamamoto et al., 2018). The steady state activity has been ascertained in volcanoes and magmatic provinces with different magmatic composition and located in different tectonic settings, although the steady state activity occurring on time scales of few decades is mainly related to mafic and intermediate composition volcanoes that more easily maintain a sustained volcanic activity over many years (Bonaccorso & Calvari, 2013; Crisp, 1984; King, 1989; Kuntz et al., 1986; Marturano et al., 2018; Wadge, 1982; Yamamoto et al., 2018). The causes of the steady state volcanism are still debated, can differ from one province to another, and might be related to multiple processes acting together at different scales, from the geodynamic scale to the local scale (Crisp, 1984; Wadge, 1982). Despite this, steady state volcanism has implicit implications for the

evaluation of volcanic hazard, since it is one of the few tools available to provide a raw estimation of the maximum expected erupted volume at the onset of an eruption (types I, II and IV; Figure 1) or, for an activity of type III (Figure 1), the duration of repose periods (Bonaccorso & Calvari, 2013; Calvari & Nunnari, 2022; King, 1989; Wadge, 1982). In this frame, type IV is significant since it provides the maximum volume that can be erupted by paroxysmal periods following longer repose times (or times with low erupting rates), as done multiple times at Mt. Etna (Figure 2), although it is not possible to forecast the time of onset of the paroxysm (Bonaccorso & Calvari, 2013; Calvari et al., 2020; Calvari & Nunnari, 2022; Harris et al., 2011; Wadge, 1982; Wadge & Guest, 1981). Type IV behaviour has been called size-predictable, while type III behaviour is time-predictable (e.g., Bebbington, 2014; De la Cruz-Reyna, 1991). Thus, a better understanding of steady state volcanism, and of how common types IV and III are, has implications for volcanic hazard evaluation, particularly the challenging problem of forecasting eruption size (Bebbington, 2014).

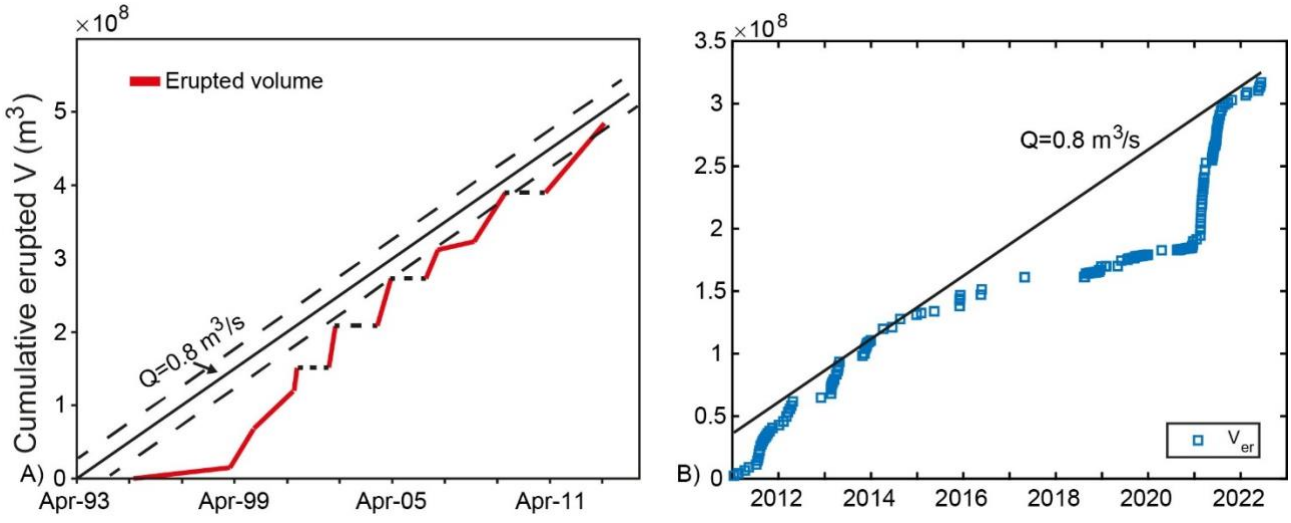

Figure 2. Example of the well-constrained steady state activity at Mt. Etna (Italy) from 1993 to 2013 (panel A modified from Bonaccorso & Calvari, 2013) and from 2011 to 2022 (panel B; data from Calvari & Nunnari, 2022). The steady state activity at Etna started since 1971 at constant rates of ~0.8 m³/s (back line). Dashed lines in panel a represent the uncertainties (standard deviation) associated with the steady state rates (see Bonaccorso & Calvari, 2013).

Despite the advance in the methods to evaluate the erupted volumes, steady state activity has not been deeply analysed and investigated in the last couple of decades, especially in the magmatic provinces. Thus, to increase the knowledge on steady state volcanism, here we investigated the steady state activity in four frequently erupting and well-studied oceanic hot spots (Iceland, La Réunion, Hawai'i and western Galápagos). In two of them (Iceland and western Galápagos) the volcanism is widespread, and we consider the volumes erupted by all their volcanoes to see if the steady state

activity exists at the level of the magmatic province, reflecting a possible steady state regime of the hot spot. In the other two hot spots (Hawai'i and La Réunion) the volcanism is localized, and the steady state regime was previously identified (e.g., King, 1989; Staudacher et al., 2016). These four hot spots provide ideal case studies to investigate the steady state volcanism since they erupt frequently and have constrained erupted volumes for many decades, allowing to build curves of cumulative erupted volume for long periods. Furthermore, here we can also investigate the relationship between the present steady state rates and the longer-term ($\geq 10^3$ yr) rates. Steady-state rates can provide an estimation of the maximum expected erupted volume (Bonaccorso & Calvari, 2013; Calvari & Nunnari, 2022; Wadge, 1982), and we used two simple methods to quantify how well steady-state rates hindcast the erupted bulk volumes of each eruption, providing an estimation of the difference between the true erupted volume of each eruption and the expected maximum erupted volume from steady state rates. Although outside the main aims of this work, when possible, we also included the volume of magma that remained intruded into the propagating dikes and sills to understand if some decrease in the observed erupted volumes can be related to higher intruded volumes.

2) Methodology

2.1 Dataset building

The erupted bulk and Dense Rock Equivalent (DRE) volume of magma come from previously published data (the list of these references is provided in the data availability statement, in the **S**upplementary Material and in the Supplementary Tables S1-S4). In Supplementary Tables S1-S4 we reported also the porosity assumed to convert the bulk volume in DRE (and vice versa) used by the published articles, as well as the one that we used for these conversions for the cases where previously published articles reported only the bulk or the DRE volume. In Supplementary text S1 and Figure S1, we report how we estimated the volumes of the 1979 and the 2008 eruptions at Cerro Azul (Galápagos), not available in previously published data. The dataset shows the erupted volumes up to 2023, with the exceptions of Iceland and western Galápagos for which we found also the volumes erupted in 2024.

Although the primary aim of this work is the analysis of the steady state volcanism, and thus of the erupted volumes, when possible we also reported the intruded volumes, which however in most cases do not provide us a complete dataset, and thus we used this information just to identify possible relationship between reductions in the eruptive rates and increase in the intruded volumes for some periods. The intruded volume here is meant as the volume intruded into dikes and sills propagating

outside the magma chamber during eruptions or intrusive events, and not as the volume of magma accumulated into the magma chamber in the inter-eruptive periods. The intrusive volumes here considered come from the inversion of geodetic data using elastic models and thus is considered as DRE volume (Chadwick et al., 2011; Wauthier et al., 2015; see also Supplementary Text S2). As for Hawai‘i, which is characterized by a complex intrusive history analysed by previous studies (Dvorak & Dzurisin, 1993; Dzurisin et al., 1984; Montgomery-Brown & Miklius, 2020; Poland et al., 2014; Wright & Klein, 2014), we do not report the intruded volumes, since it would require a detailed analysis that is beyond the aims of this work. However, we discuss how the observed steady state rates at Hawai‘i are affected by the intruded volumes, based on the results of the previous studies about intruded volumes at Hawai‘i (Dvorak & Dzurisin, 1993; Dzurisin et al., 1984; Montgomery-Brown & Miklius, 2020; Poland et al., 2014; Wright & Klein, 2014).

2.2 Steady state volume prediction and statistical tests.

We applied two methods to evaluate the ability of steady-state rates to hindcast, and potentially forecast, the erupted bulk volumes (which are the better constrained volumes) of the four analysed hot spots during the studied time periods. The average steady-state rate (Q) is computed from the time series of cumulative volumes as (1):

$$Q = \frac{\Delta V}{\Delta t} \qquad (1)$$

where Δt is the total time span of the analysed period, and ΔV is the total cumulative volume erupted within this time. The rates for the four analysed hot spots are reported in Figures 3-6.

The first method, hereafter referred to as the *Q-line fitting* method, employs the average steady-state rate (Q) from Equation (1) to linearly extrapolate the expected cumulative bulk volumes over a given period. The difference between the hindcasted and observed values quantifies the error, which is graphically represented by the distance (along the y-axis direction) from the Q-line to the observed data (see Figure 7). The second approach, referred to as the *deterministic time interval* method, is based on the following linear state equation, obtained by rearranging equation (1):

$$V_2 = Q\,(t_2 - t_1) + V_1 \qquad (2)$$

Where Q is the average steady-state rate of the studied period (from equation 1), and V_1, V_2 are the cumulative bulk volumes after the eruptions that ended by time t_1 and t_2, respectively (see also Supplementary Text S3 for La Réunion). By knowing Q, V_1, and the time interval between t_1 and t_2 for the eruptions in our dataset, it is possible to hindcast the cumulative volume V_2 resulting from the eruption that ends by time t_2. The error is again given by the difference between the calculated and

observed cumulative volumes (see Figure 8). For both methods, we show the following error metrics: mean, standard deviation, and distribution (as a discrete histogram). The mean error quantifies systematic bias in the estimates, while the standard deviation quantifies the variability of the error across samples. The error distribution characterizes the shape and spread of the errors beyond what is captured by aggregate metrics, enabling evaluation of symmetry, tail behaviours, and the presence of outliers. Additional computed parameters and individual estimates are included in the Supplementary Text S4 and Supplementary Tables S5-S6.

3) Steady state hot spots results

3.1 Hot spots with widespread volcanism

3.1.1 Iceland

In Figures 3A-B, we show the cumulative bulk (Figure 3A) and DRE (Figure 3B) volume of magma erupted in Iceland from 1961 (Askja eruption) to December 2024. These volumes have been compared with the longer-term average eruptive rates (bulk and DRE) estimated for about the last millennium in Iceland by Thordarson & Larsen (2007) (Figures 3A-B). We observe that over the decadal analysed time span, there is an overall good relation between the erupted volumes and the longer-term eruptive rates, although the cumulative erupted volume over time often shows type IV steady state activity, with periods characterized by rates lower than the average, followed by periods with eruptive rates higher than the average that recover most (or all) of the volume not erupted in the periods with lower rates (Figures 3A-B). A type IV cycle here in Iceland can last also for decades. For example, we observe that the 2011 eruptions at Eyjafjallajökull and Grímsvötn and the 2014-2015 Bárðarbunga eruption followed a long period characterized by rates lower than the average and re-equilibrated the cumulative erupted volumes of Iceland with the ones expected from the longer-term rates (Figures 3A-B). The Bárðarbunga eruption was followed by years with rates lower than the average, with the Fagradalsfjall and Sundhnúkur eruptions that up to November 2024 have not yet re-equilibrated the cumulative erupted volumes of Iceland with the ones expected from longer-term rates, suggesting that Iceland might still be in a type IV cycle. Indeed, the total average bulk and DRE eruptive rates from 1961 to November 2024 are of ~0.102 km^3/yr and of ~0.069 km^3/yr, respectively, which are slightly lower than the average longer-term bulk and DRE rates of ~0.111 km^3/yr and of ~0.079 km^3/yr estimated by Thordarson & Larsen (2007) (Figure 3A-B). Since volcanoes in Iceland are placed within well-developed rift zones (Thordarson & Larsen, 2007), the propagation of magma often occurs through well-developed vertical dikes that do not necessary

intercept the topography triggering an eruption, as occurred multiple times during the 1975-1984 eruptive cycle at Krafla and the 2023-2024 eruptive cycle at Sundhnúkur (Parks et al., 2025; Tryggvason, 1984, 1986). Thus, for the four cases (Krafla, Bárðarbunga, Fagradalsfjall and Sundhnúkur) where the intruded volumes are known, we added to the erupted volume also the volume intruded as dikes, regardless of whether the dike triggers the eruption or not (Figure 3C). The addition of the intruded volumes for these four periods reveals some interesting patterns. For example, during the Krafla eruption (1975-1984), the period 1975 - July 1980 is characterized by eruptive rates lower than the steady-state rates (Figure 3A-B) because this period was dominated by intrusions (Tryggvason, 1984). By considering also the volumes intruded as dikes, the type IV activity observed from 1975 to 1984 in the cumulative erupted volumes (Figure 3A-B) becomes a type I – type II activity (Figure 3C). Furthermore, we observe that the type IV activity from November 2023 to November 2024 becomes more evident (Figure 3C) once we consider also the important volumes intruded as dikes during the Sundhnúkur intrusive-eruptive sequence (Parks et al., 2025). Thus, although our dataset of intrusive volumes is incomplete, the available data suggest that the steady-state behaviour remains confirmed, and likely even more evident, by considering the erupted plus intruded volumes. Due to the incompleteness of the dataset of the intruded volumes, the average intruded plus erupted rates of ~0.1 km^3/yr in Figure 3C is a lower estimation. Future studies should better constrain the erupted + intruded V at Iceland.

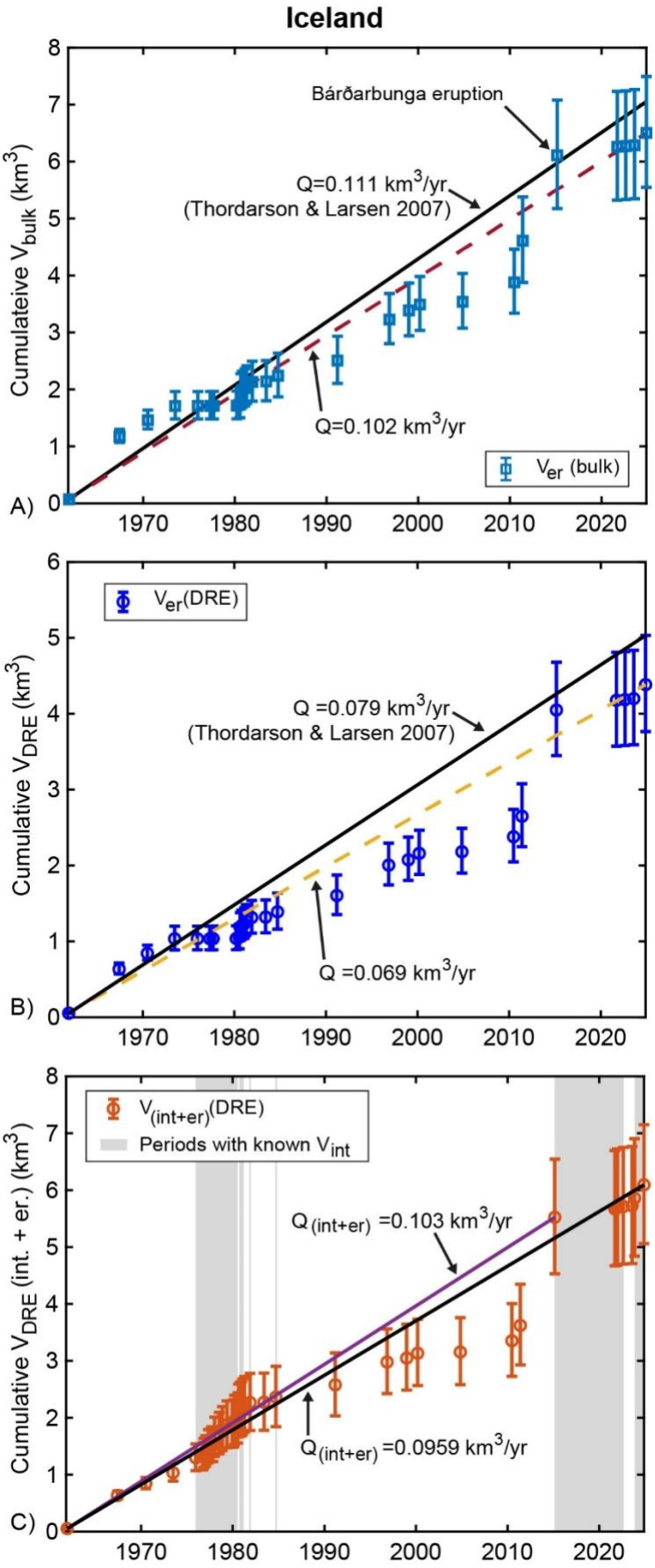
Iceland
Bárðarbunga eruption
Q=0.111 km3/yr
(Thordarson & Larsen 2007)
Q=0.102 km3/yr
Ver (bulk)
Cumulateive Vbulk (km3)
A)
Ver(DRE)
Q =0.079 km3/yr
(Thordarson & Larsen 2007)
Q =0.069 km3/yr
Cumulative VDRE (km3)
B)
V(int+er)(DRE)
Periods with known Vint
Q(int+er) =0.103 km3/yr
Q(int+er) =0.0959 km3/yr
Cumulative VDRE (int. + er.) (km3)
C)
1970
1980
1990
2000
2010
2020

212

Figure 3. A-B) Cumulative erupted bulk (panel A) and DRE (panel B) volumes of magma in Iceland. The black lines in panels a-b are the average bulk (panel A) and DRE (panel B) erupting rates inferred by Thordarson & Larsen (2007) for about the last millennium. Red and yellow dashed lines in panels A and B are the average bulk and DRE erupting rates from 1961 to 2024, respectively. C) Total cumulative volumes of erupted plus intruded (in the dikes) magma. The intruded volumes are constrained only for the periods within the grey areas. The violet and the black lines represent the average intrusive plus eruptive rates from 1961 to 2015 and from 1961 to 2024, respectively. These rates however are poorly constrained, since intruded volumes are known only for a few periods. Data and associated references are reported in Supplementary Table S1.

3.1.2 Western Galápagos (Ecuador)

The western Galápagos volcanoes on Isabela and Fernandina islands make up a distinct magmatic province with respect to the eastern Galápagos volcanoes (Geist et al., 2014; Harpp & Geist, 2018). Thus, in this analysis we consider only the volumes erupted at the western Galápagos volcanoes, which are the most active. Contrary to the other analysed hot spots, the erupted volumes at western Galápagos volcanoes are constrained only for the last decades (Figure 4; Supplementary Table S2). Despite this, from 1988 to present, the cumulative erupted volume suggests that also the western Galápagos are experiencing steady state activity, with some observed type IV behaviours, at rates of ~0.025 km^3/yr (bulk volume; Figure 4A), equivalent to ~0.018 km^3/yr DRE (Figure 4B). These rates are higher than the longer-term (10^3-10^5 yr) rates of 0.0086±0.0018 km^3/yr (Figure 4B), although these latter are not well-constrained (Galetto, Pritchard, et al., 2023; Geist et al., 1994; Geist, 1996; Geist et al., 2005; Kurz et al., 2014; Naumann & Geist, 2000; Reynolds et al., 1995). Figures 4A-B show a large jump in the erupted volume in 1980 due to the large 1979-1980 eruption at Sierra Negra. Without an accurate knowledge of the volume erupted at the western Galápagos volcanoes before 1979, and from 1980 to 1988, it is difficult to understand whether this eruption is related to a type III or IV steady state activity, or if it has been an out of trend event not connected with the steady state behaviours. For the same reason, it is not possible to know if the 1979-1980 eruption at Sierra Negra also caused a change in the steady-state rates.

The volume that remains intruded in dikes (or lateral sills) during eruptions at Western Galápagos volcanoes is often significant, with some events that are also only intrusive (Bagnardi & Amelung, 2012; Galetto, 2023; Galetto et al., 2020; Galetto, Reale, et al., 2023; Guo et al., 2019). Since 1995 the intruded volumes have been estimated for all eruptions, except for the eruptions at Cerro Azul in 1998, at Sierra Negra in 2005 and the last eruption at Fernandina in 2024 (Supplementary Table S2). Figure 4C shows the total cumulative volumes of erupted plus intruded magma, with the steady state

activity that remains confirmed. Even in this case the calculated average extruded plus intruded rates of ~0.03 km^3/yr are a minimum estimation due to the lack of three intruded volumes (Figure 4C).

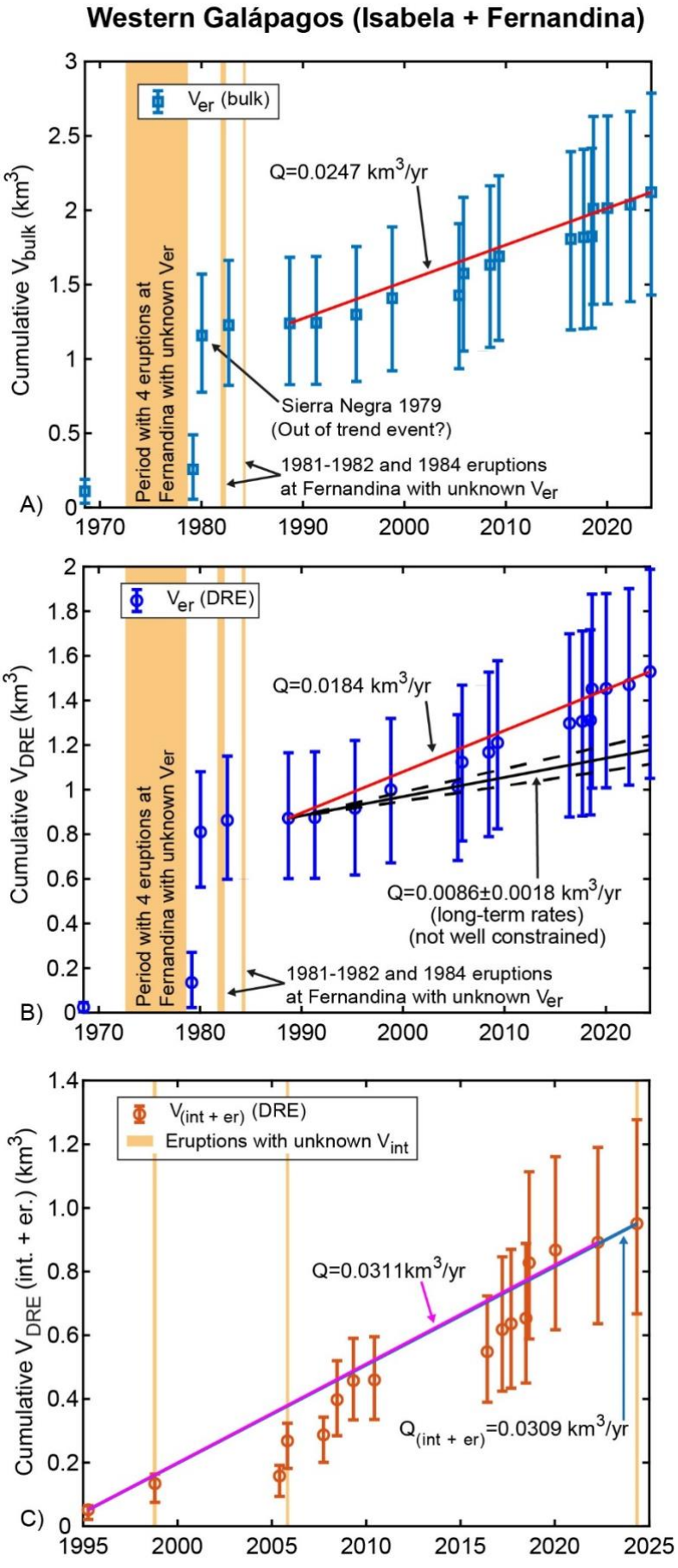
Western Galápagos (Isabela + Fernandina)
A)
Cumulative V_{bulk} (km^3)
V_{er} (bulk)
Q=0.0247 km^3/yr
Period with 4 eruptions at Fernandina with unknown Ver
Sierra Negra 1979
(Out of trend event?)
1981-1982 and 1984 eruptions at Fernandina with unknown V_{er}
B)
Cumulative V_{DRE} (km^3)
V_{er} (DRE)
Q=0.0184 km^3/yr
Q=0.0086±0.0018 km^3/yr
(long-term rates)
(not well constrained)
Period with 4 eruptions at Fernandina with unknown Ver
1981-1982 and 1984 eruptions at Fernandina with unknown V_{er}
C)
Cumulative V_{DRE} (int. + er.) (km^3)
$V_{(int + er)}$ (DRE)
Eruptions with unknown V_{int}
Q=0.0311km^3/yr
$Q_{(int + er)}$=0.0309 km^3/yr

248

Figure 4. A-B) Cumulative erupted bulk (panel A) and DRE (panel B) volume of magma from western Galápagos volcanoes. Red lines in panels a and b are the average bulk and DRE erupting rates from 1988 to 2024, respectively. The black lines in panel b represent the longer-term (10^3-10^5 yr) eruptive rates estimated for the western Galápagos by previous authors (see text in section 3.1.2). C) Cumulative total volume (DRE) of magma erupted and intruded (as dikes) in western Galápagos. The blue and purple lines are the average intrusive plus eruptive rates estimated from 1995 to 2024 and from 1995 to 2022 (excluding the 2024 eruption at Fernandina with unknown intruded volumes), respectively. Data and associated references in Supplementary Table S2.

3.2 Hot spots with localized volcanism

3.2.1 La Réunion (Piton de la Fournaise)

The magmatic activity at La Réunion is currently focusing on Piton de la Fournaise volcano, which has a known steady state activity (Campus et al., 2025; Staudacher et al., 2016; Vlastélic et al., 2018; Wadge, 1982). In Figure 5A-C, we show the cumulative erupted bulk (Figure 5A-B) and DRE (Figure 5C) volumes from 1931 to 2023 (data and references in Supplementary Table S3). This long dataset allowed us to study two episodes of steady state activity characterized by different steady-state rates: one from August 1936 to March 1998 and the second one from July 1999 to July 2023 (Figure 5A-C). The first episode shows all types of activity (I-IV) of steady state volcanoes (Figure 5A,C). In detail, we observe a few minor type III activities, connected for example with the December 1938 and the April 1961 eruptions (Figure 5A,C), and multiple type IV activities that became dominant especially during the period 1972-1982 that followed a period of six years of quiescence (Peltier et al., 2009). We calculated average bulk steady state rates of the first episode (1936-1998) of 0.011 km^3/yr (Figure 5A). The corresponding DRE steady state rates of the first episode are of 0.006 km^3/yr (Figure 5C). The second episode is characterized by an increase in the average steady state rates, well documented by previous studies (e.g., Peltier et al., 2009, 2018; Staudacher et al., 2016; Vlastélic et al., 2018). We calculated for the second episode bulk steady state rates of 0.022 km^3/yr from 1999 to 2023 (DRE rates of 0.013 km^3/yr; Figure 5C) and of 0.023 km^3/yr (0.014 km^3/yr DRE) from 1999 to April 2020, which provides a slightly better fitting of the data (Figure 5B). The second episode is characterized by type III behaviour. Indeed, after about 9 years (July 1999-March 2007) of type I-II steady state activity, an out of trend eruption occurred at the beginning of April 2007 (the caldera collapse eruption; Figure 5). This eruption, however, was followed by 7 years of eruptive rates significantly lower than the steady state rates, leading to a re-equilibrium of the erupted volumes with

those expected by the steady state rates (type III behaviour, Figure 5). Then, the eruptive rates returned comparable to the steady state rates (Figure 5). Piton de la Fournaise has also a dataset of the intruded volumes that allows to calculate the total intruded plus erupted DRE volumes up to December 2020 (Derrien, 2019; Dumont et al., 2022; Figure 5C-D). The steady state activity remains confirmed, with intruded plus erupted DRE rates of 0.008 km^3/yr for the first episode and of 0.018 km^3/yr for the second episode computed from 1999 to December 2020 (last date with well constrained intruded volume).

Finally, both episodes show steady state rates higher than the long-term ($2x10^6$ yr) eruptive rates of 0.0024 km^3/yr constrained by Gerlach (1990), and also reported in White et al., (2006), which however are mainly based on an older dataset compiled from 1969 to 1972 (Gerlach, 1990).

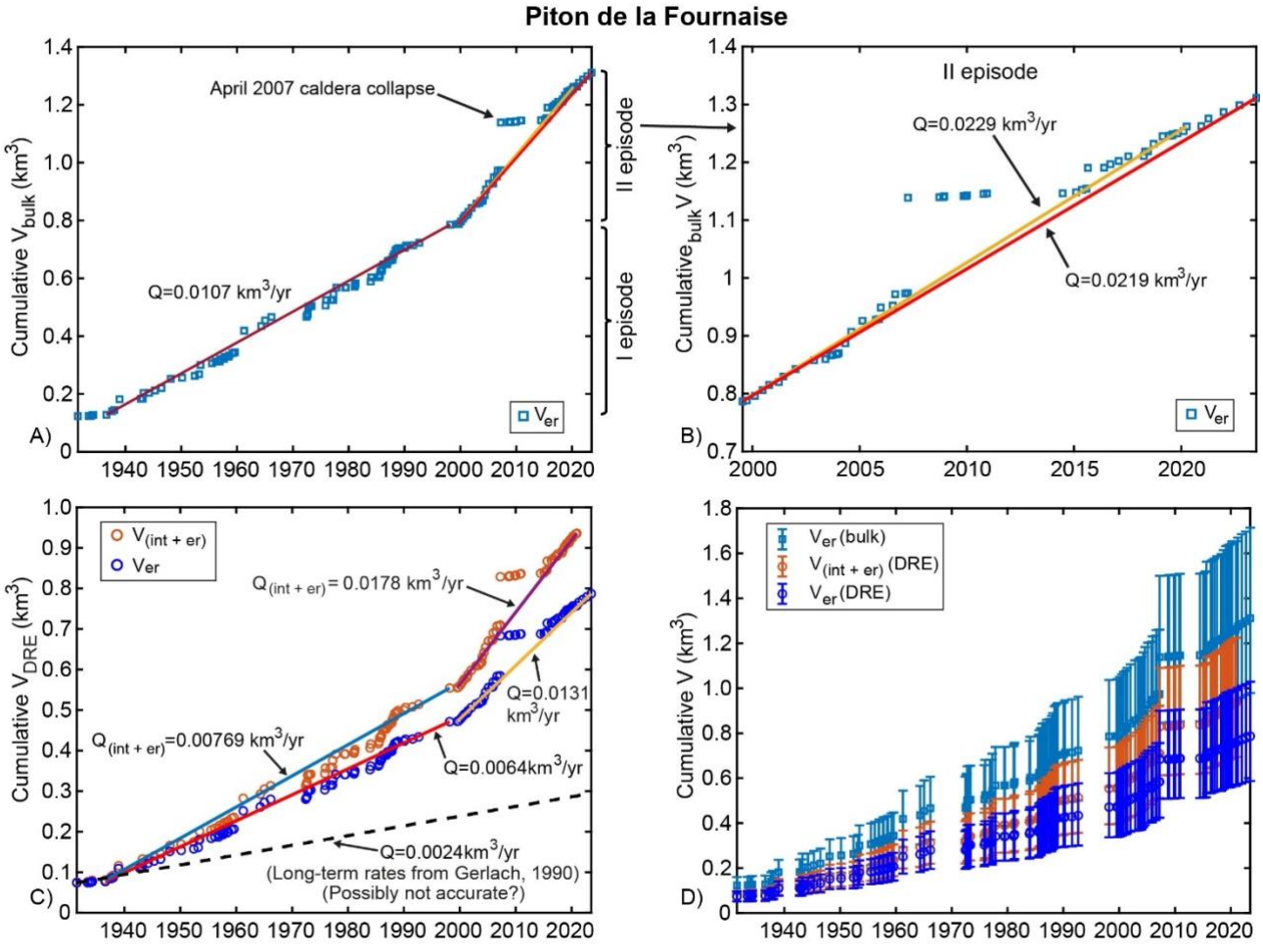

Figure 5. A-B) Cumulative erupted bulk volumes of magma at Piton de la Fournaise (La Réunion). The dark red line (panel A) represents the average rates 1931 to 1998, while the yellow and red lines (panels A-B) represent the average rates calculated from 1999 to April 2020 and from 1999 to 2023, respectively. Panel b shows a zoom of the cumulative bulk volumes erupted during the II episode

(1999-2023). C) Cumulative DRE volumes of erupted magma (blue dots) and of intruded (int) plus erupted (er) volumes (orange dots). The red and yellow lines represent the average DRE steady state rates from 1931 to 1998 and from 1999 to 2023, respectively. The blue and violet lines represent the average DRE intruded plus erupted rates from 1931 to 1998 and from 1999 to December 2020 (date with the last well constrained intruded volume), respectively. D) Errors associated with data in panels A-C. Data and associated references reported in Supplementary Table S3.

3.2.2 Hawai'i (USA)

The current hot spot volcanic activity in Hawai'i focuses on the volcanoes of Kīlauea and Mauna Loa. Steady state activity in Hawai'i was previously identified from the 1920s to the 1980s (Dvorak & Dzurisin, 1993; Dzurisin et al., 1984; King, 1989). Here we collected the volumes erupted in Hawai'i from 1903 to 2023, although some volumes erupted at Kīlauea from 1903 to 1918 are unknown (Figure 6). From 1993 to 2018, it has been more difficult to compile the year-by-year erupted volumes from available published data and therefore we just reported the total volumes erupted during the time intervals defined by Orr et al., (2015) and Neal et al., (2019). This fact, however, does not affect our results, since it still allowed us to investigate the cumulative total erupted volumes that are the target of the analysis of the steady state volcanism. The cumulative bulk (Figure 6A-C) and DRE (Figure 6D) erupted volumes shows that the steady state activity of Hawai'i can be divided in two main episodes: from August 1923 to the 1984 Mauna Loa eruption (Figure 6B) and from 1984 (after the Mauna Loa eruption) to 2023 (Figure 6C). The first episode was characterized mainly by consecutive events of type IV activity (Figure 6B). The predominance of the type IV activity during this episode can be related also to the intruded volumes that have been important during some periods characterised by low eruptive rates, such as the 1977-1980 (see details in Dvorak & Dzurisin, 1993; Dzurisin et al., 1984; Heliker & Mattox, 2003; Klein et al., 1987; Wright & Klein, 2014). For the first episode, we calculated average bulk and DRE steady state rates of 0.04 km^3/yr and 0.03 km^3/yr, respectively (Figure 6). The first period ended in April 1984, with the volumes erupted by the onset of the 1983-2018 eruption at Kīlauea and with those erupted by the 1984 eruption at Mauna Loa. After the 1984 Mauna Loa eruption, the volume of extrusive material erupted at Hawai'i until 2018 was erupted continuously by Kīlauea volcano during the 1983-2018 eruption, characterized by average eruptive rates higher than those of the previous episode (Dvorak & Dzurisin, 1993; Orr et al., 2015; Wright & Klein, 2014). We calculated for the second episode (1984-2023) average bulk and DRE steady state rates of ~0.19 and ~0.14 km^3/yr, respectively (Figure 6). These rates are significantly higher than those of the first episode. However, a detailed analysis of the

eruptive rates of the second episodes reveals further changes (Figure 6C). Indeed, the average bulk rates have been of ~0.13 km^3/yr (~0.09 km^3/yr DRE) up to 1993 and then increased from 1993 to December 2022 (~0.2 km^3/yr bulk and ~0.15 km^3/yr DRE). The rates slightly slowed down again in 2023, which might hint also to the beginning of a type IV activity or of a new episode. It is interesting to note that the 2018 eruption at Kīlauea shows behaviours of both type III and IV (Figure 6C). Indeed, this large eruption was preceded by a period with rates lower than the steady state rates (type IV), but it erupted more magma than expected and was followed by a quiescent period proportional to the "excess" volume (type III).

Steady state rates of the first and second episodes are respectively lower and almost equal than the combined Kīlauea and Mauna Loa long-term eruptive rates (0.14 km^3/yr) reported in White et al., (2006) for the last 0.4-0.5 million years (Figure 4C), and respectively lower and higher than the combined Kīlauea and Mauna Loa eruptive rates of 0.07 km^3/yr estimated for the last kiloyears (Figure 6D; Lipman, 1995; Quane et al., 2000).

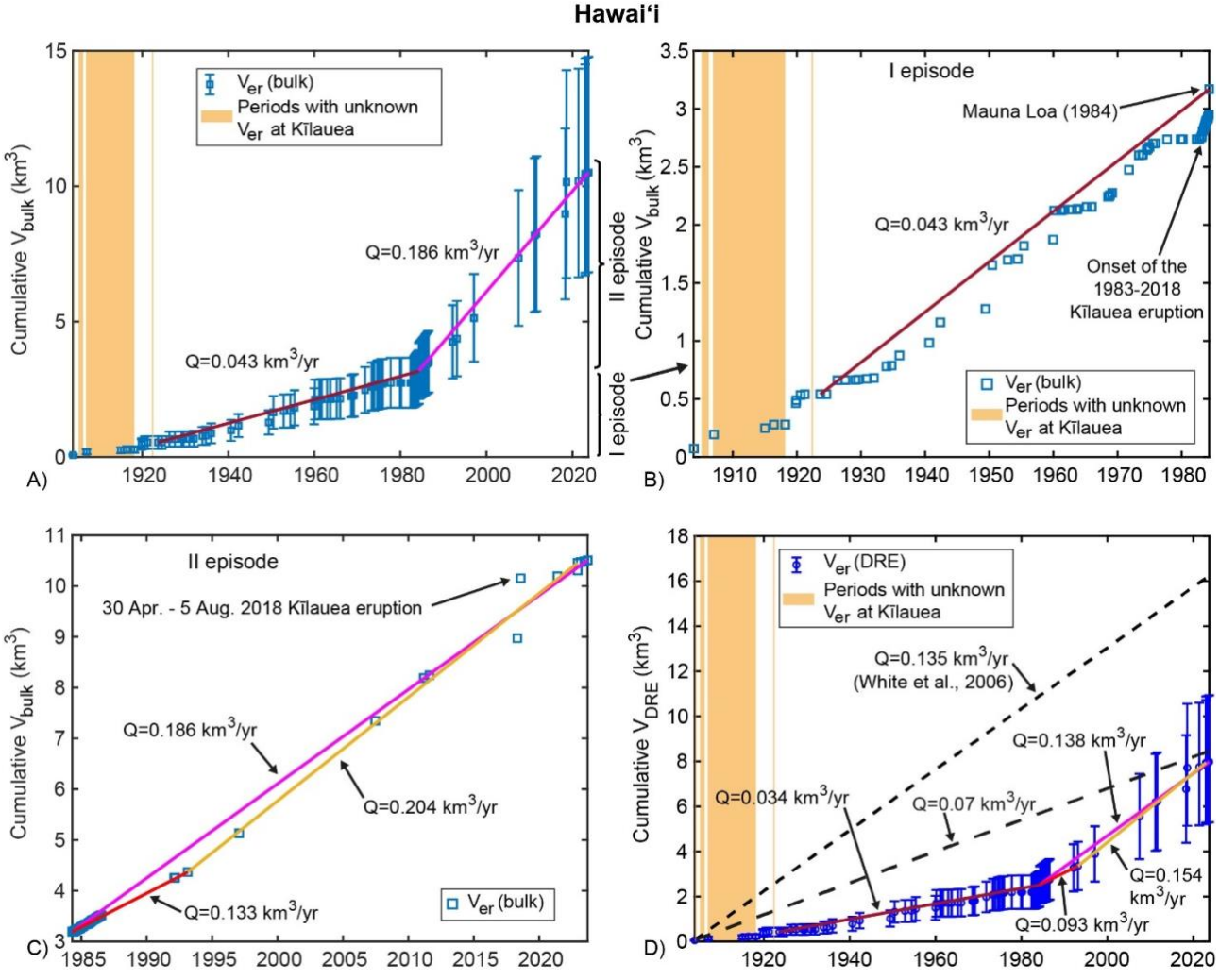

Figure 6. Cumulative bulk (panels A-C) and DRE (panel D) volumes of magma erupted in Hawai'i. Panel b and c show a subset of the data in panel a, with panel b showing the data from 1903 to the 1984 Mauna Loa eruption (thus including the I episode) and panel c data from 1984 (after the Mauna Loa eruption) to 2023 (II episode). Dark red and magenta lines are the average steady state of the I (1923-1984) and II episode (1984-2023) respectively. Red and yellow lines show the average rates from 1984 to 1993 and from 1993 to 2022 respectively. Dashed lines in panel d are the eruptive rates reported in White et al., (2006) for the last millions of years (0.135 km^3/yr) and in Lipman (1995) for the last kiloyears (0.07 km^3/yr). Data and associated references in Supplementary Table S4.

4) Steady state cumulative bulk volumes prediction results

Analysis of historical eruption data shows that individual bulk erupted volumes and the intervals between consecutive eruptions consistently display right-skew normal characteristics (O'Hagan & Leonard, 1976), across all studied periods and hot spots (Supplementary Figures S2–S6). This indicates that the data conform to a relatively well-behaved statistical distribution. Additionally, when considering the cumulative erupted volumes over time, the data align with fitting lines whose slopes correspond to the average steady-state rates (Figures 7-8), a pattern that is encouraging for predictive applications. Building on this empirical characterization, we applied the two methods described in Section 2.2 to evaluate their ability to predict cumulative bulk volumes from the steady-state equation. Supplementary Table S5 reports the results obtained using both methods for each eruption, and Supplementary Table S6 provides a comparison of error statistics for the two methods across the four analysed hot spots (see Supplementary Text S4 for calculation details).

Figure 7 shows the results obtained with the *Q-line fitting* method (see Section 2.2, Equation 1). As expected, for each analysed hot spot this method yields lower errors (difference between the cumulative erupted and expected volumes) during type I and II activity, and higher errors during types III and IV activity, since they mark a shift from the linear behaviour (Figure 5; Supplementary Tables S5-S6). Although the error between the expected and the erupted volume of an eruption can be high during periods with activity of type III and IV, it is important to note that in all the analysed cases the error decreases again by the end of the corresponding type III or IV cycle (Figure 7B,E,H,K). This pattern is consistent with rebalancing of erupted volumes relative to steady-state rates over time. When estimation errors arise from many independent random contributions and can therefore be viewed as the sum of multiple random variables, the central limit theorem predicts that their distribution approaches a Gaussian (Walker, 1969). Under this assumption, error distributions that more closely resemble a zero-mean Gaussian are commonly associated with better estimation performance. In this context, hot spots dominated by pronounced type IV activity (e.g., Iceland and

the western Galápagos) exhibit error distributions with stronger deviations from a zero-mean Gaussian, including a higher prevalence of outliers (Figure 7C and 7F). By contrast systems with type I-II activity or type IV activity that often remains closer to the steady state-rate (e.g., Piton de la Fournaise, Figure 7I) show error distributions closer to Gaussian behaviour, with more stable model performance.

Figure 8 shows results of the *deterministic time interval* method (see Section 2.2, Equation 2), which outperforms the previous method in forecasting cumulative erupted volumes (Figure 8; Supplementary Table S5). Although periods associated with the largest departures from steady behaviour (points of maximum shift during type III-IV activity) still exhibit high errors (Figure 8), these are often lower than those encountered with the *Q-line fitting method* (Figure 7-8; Supplementary Table S5). Overall, the error distribution for all analysed hotspots increasingly approaches a zero-mean Gaussian (Figure 8C,F,I,L), with some negative skewness caused by significant type III activity (e.g. Piton de la Fournaise, Figure 7I and 8I). When errors are normalized by the total cumulative erupted volume to account for differences the in total erupted volume among hotspots (Supplementary Table S6), the estimation error in both methods increases in the following order: Hawai‘i, Piton de la Fournaise, Iceland, and the western Galápagos (Supplementary Table S6). Note that the method performance might also be influenced by differences in data availability across hotspots, with more extensive eruptive records for systems such as Hawai‘i and Piton de la Fournaise (Supplementary Table S6).

We also tested the two methods by using the rates computed for the second episode at La Réunion from 1999 to April 2020 (Figure 5B; Supplementary Figure S7) and at Hawaii by dividing the second episode in two parts (1988-1993 and 1993-December 2022; Figure 6C; Supplementary Figure S8). Results show a decrease in the errors of the predicted volumes with the *Q-line fitting* method due to a better linear fitting by using the average rates constrained in these time spans, while the *deterministic time interval* method produced similar results (Supplementary Figures S7-S8, Supplementary Tables S5-S6).

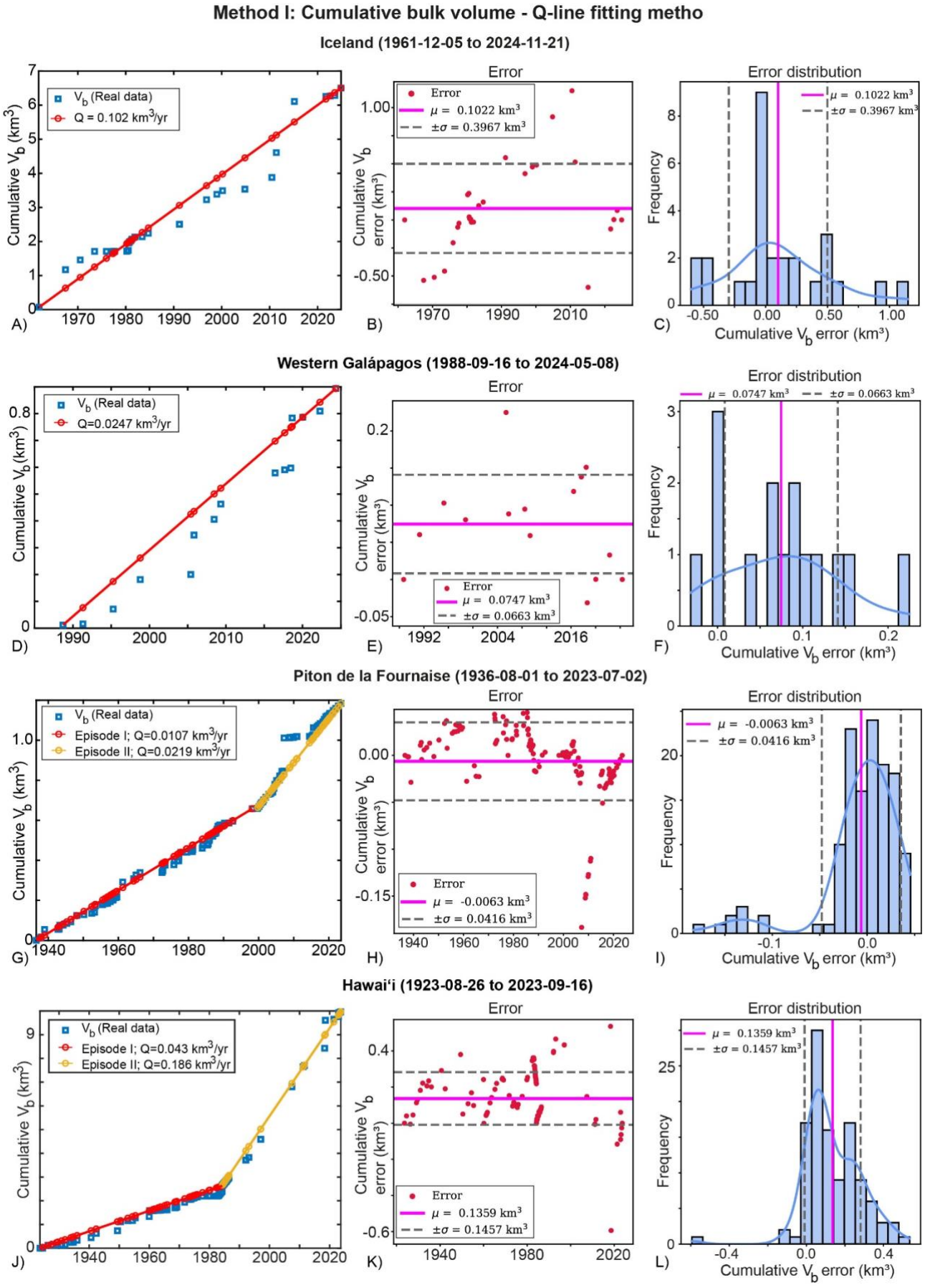
Method I: Cumulative bulk volume - Q-line fitting metho
Iceland (1961-12-05 to 2024-11-21)
Western Galápagos (1988-09-16 to 2024-05-08)
Piton de la Fournaise (1936-08-01 to 2023-07-02)
Hawai'i (1923-08-26 to 2023-09-16)
Error
Error distribution
Frequency
Cumulative V_b error (km³)
A)
B)
C)
D)
E)
F)
G)
H)
I)
J)
K)
L)

403

Figure 7. A,D,G,J) Expected cumulative bulk volumes (red and orange dots) obtained with the Q-line fitting method (method I; section 2.2). B,E,H,K) Associated errors (difference between the real data and the expected ones) and their frequency distribution (panels C,F,I,L).

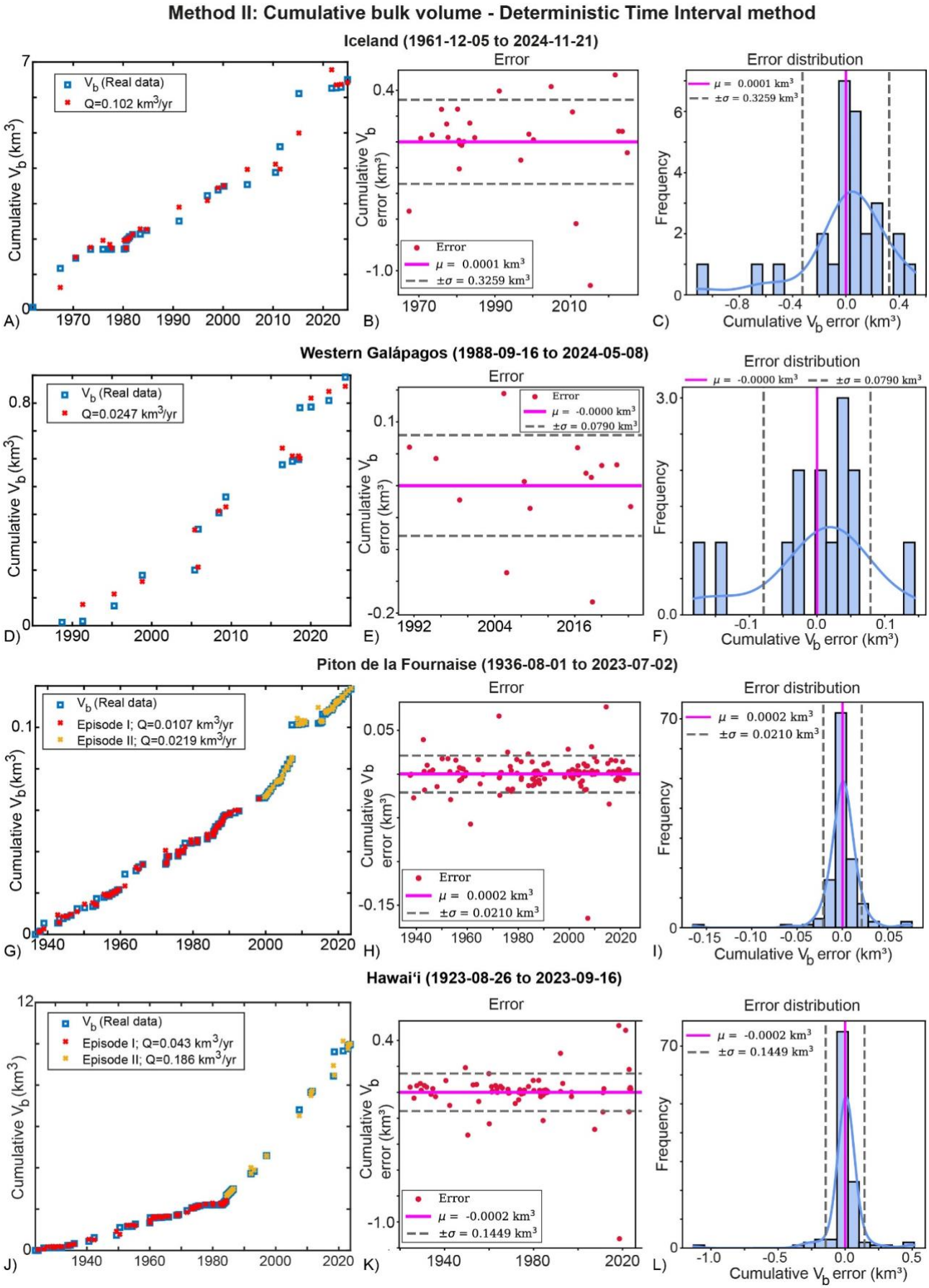
Method II: Cumulative bulk volume - Deterministic Time Interval method
Iceland (1961-12-05 to 2024-11-21)
Western Galápagos (1988-09-16 to 2024-05-08)
Piton de la Fournaise (1936-08-01 to 2023-07-02)
Hawai'i (1923-08-26 to 2023-09-16)
Error
Error distribution
Frequency
A)
B)
C)
D)
E)
F)
G)
H)
I)
J)
K)
L)

407

Figure 8. A,D,G,J) Expected cumulative bulk volumes (red and orange cross) obtained with deterministic time interval method (see section 2.2). B,E,H,K) Associated errors (difference between the real data and the expected ones) and their frequency distribution (panels C,F,I,L).

5) Discussion

5.1) Steady state volcanism and volcanic hazard

The four analysed oceanic hot spots (Iceland, La Réunion, Hawai'i and western Galápagos), whose continuous or frequent volcanic activity is directly fed by mantle plumes, provide us ideal case studies to investigate steady state volcanism in magmatic provinces. Our data show that the analysed hot spots are in a steady state of activity, for which we calculated the bulk and DRE steady state erupting rates. At La Réunion and Hawai'i the steady state activity was previously identified (Dvorak & Dzurisin, 1993; King, 1989; Staudacher et al., 2016). In detail, at La Réunion the calculated average bulk steady state rates (0.011 km^3/yr) of the first episode (1936-1998) are consistent with the rates of 0.010 km^3/yr calculated by Staudacher et al., (2016) for the period 1950-1998. On the contrary, for the second episode (1999-2023) we calculated bulk steady state rates (0.02 km^3/yr) that are lower than the 0.03 km^3/yr estimated by Staudacher et al., (2016) for the period 1998-2013. This discrepancy is however mainly due to: 1) the fact that the volumes erupted in the large April 2007 eruption have been re-estimated (and lowered) after Staudacher et al., (2016) (Derrien, 2019; Peltier et al., 2018) and 2) in 2013 the cycle with the type III activity connected to the April 2007 eruption was not ended yet and thus the cumulative erupted volumes were still higher than those expected by the steady state rates that can be computed before the onset of this type III activity (Figure 5). It is important to remember that the determination of the steady state rates is indeed influenced by the arbitrary choice of the dates used to compute them (King, 1989). As for Hawaii, the bulk steady state rate (0.043 km^3/yr) of the first episode (1923-1984) is: 1) consistent with the rates of 0.04 km^3/yr estimated by Macdonald et al., (1983) for the period 1919-1982; 2) higher than the rates of 0.036 km^3/yr estimated by King (1989) for the period 1919-1984; 3) lower than 0.05 km^3/yr for the period 1823-1969 calculated by Moore (1970). The increase in the eruptive rates during the second episode was identified by previous studies, and is consistent with the studies from which we took the erupted volumes (Dietterich et al., 2021; Dvorak & Dzurisin, 1993; Heliker & Mattox, 2003; Mulliken et al., 2024; Neal et al., 2019; Orr et al., 2015; Poland et al., 2014).

The steady state activity observed in these hot spots shows all the main behaviours (type I-IV) firstly proposed by Wadge (1982), with a predominance of type IV steady state activity. The repeated

occurrence of small (possible connected also with type II) or large type IV activity observed at all the analysed hot spots suggest that the size of the next paroxysmic event is directly related to the time of the repose period (or of the period with rates significantly lower than the steady state rates), as observed also in other steady state volcanoes (Bonaccorso & Calvari, 2013; Calvari & Nunnari, 2022). Thus, the larger the period with no eruption (or characterized by low eruptive rates), the higher the possibility to have larger eruptions, with important implications in the evaluation of the volcanic hazard of these hot spots. Although type IV behaviour does not allow one to forecast the time of onset of the eruption(s) that will re-equilibrate the erupted volumes, it provides an empirical tool for forecasting the maximum size of the expected eruptions after longer repose periods (Bonaccorso & Calvari, 2013; Calvari & Nunnari, 2022). Our data show that a type IV cycle can last also for a decade or more (e.g. Iceland and Hawaii) and that the re-equilibrium can occur through multiple eruptions. For example, in Iceland the re-equilibration after the low eruptive rates that characterized the first decade of this millennium occurred in 5 years through 3 eruptions (the 2011 eruptions at Eyjafjallajökull and Grímsvötn and the 2014-2015 Bárðarbunga; Figure 3A). This is consistent with what was observed multiple times at Mt. Etna (Figure 2; Bonaccorso & Calvari, 2013; Calvari & Nunnari, 2022). The fact that the re-equilibrium between the true and the expected cumulative erupted volumes can also occur through multiple eruptions has implications for the evaluation of the volcanic hazard, since if a paroxysmic eruption does not completely re-equilibrate the erupted with the expected volumes, it is possible that future paroxysmic eruption(s) will occur to complete the re-equilibrium. For example, in Iceland the Bárðarbunga eruption was followed by years with rates lower than the average, so that the total average bulk and DRE eruptive rates from 1961 to November 2024 are of ~0.102 km^3/yr and of ~0.069 km^3/yr, respectively, which are slightly lower than the average longer-term bulk and DRE rates of ~0.111 km^3/yr and of ~0.079 km^3/yr estimated by Thordarson & Larsen (2007) (Figure 3A-B). This hints to the possibility that Iceland in November 2024 was still not in equilibrium with the expected erupted volumes from the average rates in Thordarson & Larsen (2007), potentially explaining why Iceland erupted again in 2025.

In our datasets, the type III activity is much rarer than type IV. Type III activity does not allow forecasting the expected erupted volume of the paroxysm but is however equally important since it hints to a period of no, or small, volcanic activity after the paroxysm proportional to the erupted volume (Wadge, 1982). The types I-IV behaviours have been observed in many other steady state volcanoes and magmatic provinces, with Nyamuragira and Mt. Etna providing the other two well-studied examples of steady state activity constrained over >50 years (Bonaccorso & Calvari, 2013; Burgi et al., 2021; Calvari & Nunnari, 2022; Coppola et al., 2021; Pouclet & Bram, 2021; Wadge,

1982; Yamamoto et al., 2018). Finally, we found the 2018 eruption at Kīlauea shows a mixed behaviour of type IV-III activity.

The occurrence of type III and IV activity, as well as the fact that the re-equilibration after type IV activity can occur with multiple eruptions over some years, complicates efforts to precisely forecast the size of each eruption. This is shown by the analysis in Section 4, where sometimes the predicted volumes show large errors, especially in the periods of maximum deviation from the linear behaviour during type III and IV (Supplementary Tables S5-S6). Thus, steady state volcanism does not always allow precise forecasting of the size of next eruption, but provides a powerful tool to obtain: 1) a raw estimation of the expected cumulative volumes over the decades; 2) the expected total volumes erupted by paroxysm periods (that can involve more than one eruption) in type IV activity; 3) the duration of the repose/low activity time in a type III activity. All these are valuable information for the evaluation of the volcanic hazards. Furthermore, the *Q-line fitting* and the *deterministic time interval* methods were applied here in a hindcasting framework, using the known time intervals between eruptions. However, it might also be applied in a forecasting context by simulating different possible time intervals and evaluating the corresponding expected erupted volumes.

In this study we do not present a detailed analysis of the intruded plus erupted rates, since intruded volume are usually less constrained and therefore the total (intruded + erupted) rates should be better investigated and constrained in future dedicated studies. However, some preliminary considerations can be done even from the dataset that we show in Figures 3-5 and from previously published analyses for Hawai‘i (Poland et al., 2014) and for Kīlauea in particular, since here the intruded volumes are better constrained (Dvorak & Dzurisin, 1993; Dzurisin et al., 1984; Wright & Klein, 2014). First, at Piton de la Fournaise and western Galápagos the steady state characteristics remain confirmed even by adding the intruded volumes. For Iceland we have some important gaps in the intruded volumes, but an interesting aspect is that by considering only the erupted volumes, the 1975-1984 Krafla eruption shows type IV characteristics, while by considering also the intruded volumes it shows type I characteristics (Figure 3C). On the contrary, the type IV behaviour becomes more evident (with a better re-equilibrium of the expected volumes) by considering also the intruded volumes during the 2023-2024 Sundhnúkur intrusive-eruptive sequence (Figure 3C). Also at Kīlauea previous studies show that over many decades the cumulative curves of intruded plus erupted volumes have some steady state characteristics (Dvorak & Dzurisin, 1993; Dzurisin et al., 1984), with some periods characterized by type IV eruptive activity that becomes less pronounced after the inclusion of the intruded volumes (e.g., 1960-1965; Dvorak & Dzurisin, 1993), while others maintain the type IV characteristics, with a first reduction in the total rates (lasting also for years) followed by an increase

in the total rates (see Dvorak & Dzurisin, 1993; Dzurisin et al., 1984; Poland et al., 2014; Wright & Klein, 2014).

5.2 Changes in steady state volcanism and its relationship to the long-term rates.

Hawai‘i and Piton de la Fournaise show that the steady state rates can change after many decades, starting a new episode (Figures 5, 6), similar to what was observed for Nyamuragira and Etna (Harris et al., 2011; Pouclet & Bram, 2021). While at Etna the change in the steady state rates from one episode to another one was characterized by changes in the composition, frequency and main location of eruptions (Cappello et al., 2019; Clocchiatti et al., 2004; Di Renzo et al., 2019; Viccaro et al., 2011), Piton de la Fournaise and Hawai‘i show more complex characteristics that shed light on the stability of the steady state volcanism. Vlastélic et al., (2018) associated changes in the $^{87}Sr/^{86}Sr$ and incompatible trace elements ratios of erupted lavas at Piton de la Fournaise to changes in the fertility of the mantle source that fed the volcanism, and used these changes to divide the eruptive sequence of Piton de la Fournaise from 1942 to 2017 in 4 cycles. While the passage from cycle 2 to cycle 3 identified by Vlastélic et al., (2018) is consistent with the onset of the new episode characterized by higher steady state rates, it is interesting to note how the passage among the other cycles (especially for the passage between cycle 1-2) was not characterized by changes in the steady state rates (Vlastélic et al., 2018). Similar results have been found also for Hawai‘i, where the short term (usually <10-15 years) eruptive activity has been divided in different events characterized by changes in the composition, intrusive vs extrusive volume ratio, location of the eruptions and magma supply (e.g., Dvorak & Dzurisin, 1993; Dzurisin et al., 1984; Greene et al., 2013; Heliker & Mattox, 2003; Klein et al., 1987; Poland et al., 2012, 2014; Wright & Klein, 2014). However, despite this variability on the short-term, the cumulative erupted volumes over the decades shows a steady state behaviour (King, 1989; Figure 6), with the change in the decadal steady state rates that is correlated with the occurrence of the large 1983-2018 Kīlauea eruption (Heliker & Mattox, 2003; Mulliken et al., 2024; Orr et al., 2015). Thus, the case studies of Piton de la Fournaise and Hawai‘i suggest that changes in the magmatic system do not always trigger a change in the decadal steady state rates, although these changes can affect the type of observed behaviours (type I-IV) during the steady state activity.

Future studies should also investigate whether changes in the decadal steady state rates might be considered as step changes in the longer-term (from centuries to millennia) steady state activity or not. Indeed, in some volcanoes and magmatic provinces the steady state activity has been recognized at different time scales (from decades to tens of kiloyears), despite the challenges to map, date and quantify the volume of the old deposits (Civetta et al., 1988; Jicha & Singer, 2006; Lipman, 2000;

539 Marturano et al., 2018; Nasholds & Zimmerer, 2022; Singer et al., 1997, 2008; Wadge, 1982;
540 Yamamoto et al., 2018). Thus, a future challenge would be to try building curves of cumulative
541 erupted volumes from decadal to centuries (or longer) to investigate the possible relationship between
542 the decadal and the centennial to millennial steady state activity, both at the local scale of a single
543 volcano and, although more difficult, at the regional scale of the magmatic province. At Piton de la
544 Fournaise, the steady-state rates of the two analysed episodes are higher than the long-term rates
545 estimated for the last 2 million years (Figure 5), while at Hawai'i the rates of the first and the second
546 episode are respectively lower than and almost equal to the long-term rates estimated by White et al.,
547 (2006) for the last 0.4-0.5 million years (Figure 6D). However, the estimation of rates over a such
548 long period is affected by many factors and might not be representative of the rates that occurred in
549 the last millennia (Bablon et al., 2020; Galetto, Pritchard, et al., 2023). For example, at Hawai'i the
550 average rates of 0.07 km^3/yr computed for the last kiloyears might be more representative of the
551 recent volcanic activity (Lipman, 1995; Quane et al., 2000), with these rates that also open to the
552 possibility that the two observed episodes (1923-1984 and 1984-2023) might represent a type IV
553 behaviour occurred at a longer time span (~1 century; Figure 6D). Also in Iceland we observe a good
554 consistency between the eruptive rates estimated by Thordarson & Larsen (2007) for the last 1100
555 years and the steady state eruptive rates that occurred from 1960 to present (Figure 3). These rates,
556 however, are significantly higher than the 0.02 and the 0.04 km^3/yr estimated by White et al., (2006)
557 for the last million years and the last $11x10^3$ years, respectively. Thus, a deeper analysis of the
558 eruptive rates over different time scales would be important to see if changes in the short-term steady
559 sate rates can be framed within longer term steady state periods, although these latter are more
560 difficult to estimate. Furthermore, many long-term rates have been estimated by old data, often
561 acquired between the 1960s and the 1970 (Crisp, 1984; Gerlach, 1990; White et al., 2006) and thus
562 some updates would be necessary.

563

564 *5.3) Future perspective*

565 Due to the relationship between steady state volcanism and volcanic hazards, it is important to
566 identify volcanoes and magmatic provinces that are experiencing steady sate volcanism. Recently
567 developed methods allow the improved estimation of the erupted volumes including the use of remote
568 sensing data that allows for near global monitoring (Bagnardi et al., 2016; Coppola et al., 2009, 2017,
569 2021, 2022; Dai & Howat, 2017; De Beni et al., 2021; Galetto et al., 2024, 2025; Harris et al., 2007;
570 Kubanek et al., 2015; Plank et al., 2023; Ripepe et al., 2013; Shevchenko et al., 2021).

Another important goal is to extend the analysis of the steady state activity to other magmatic provinces. Here we focused on oceanic hot spot magmatic provinces, which provide an ideal case study since they erupt frequently with well-constrained erupted volumes. More difficult is the identification of steady state volcanism in arcs. In figure 9, we used data from Galetto, Pritchard, et al., (2023) to show some arcs (the Alaska – Aleutian and the Central America arcs) that might be experiencing steady state activity. However, for many arcs the analysis of possible steady state volcanism should be performed over time span longer than the 40 years analysed by Galetto, Pritchard, et al., (2023), due to the nature of volcanism characterizing many arcs, with quick large explosive eruptions and long quiescent times.

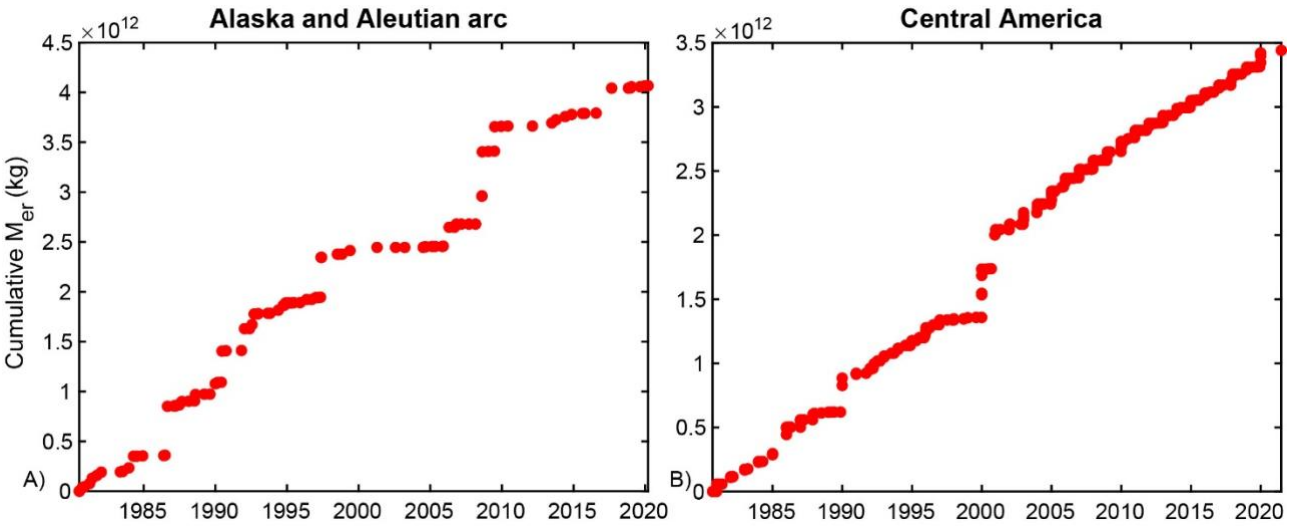

Figure 9. Cumulative masses erupted along the Alaska – Aleutian arc (panel A) and along the Central America arc (panel B) from 1980 to 2019 using data in Galetto, Pritchard, et al., (2023). Central America here includes volcanoes in Guatemala, El Salvador, Honduras, Nicaragua and Costa Rica.

6) **Conclusions**

Here we show that Iceland, La Réunion, Hawai'i and the western Galápagos volcanoes are all experiencing steady state eruptive activity for decades, despite the fact that while volcanism in Iceland and western Galápagos is distributed, at La Réunion and Hawai'i the volcanism is localized. Understanding the steady state regime is important, since it provides an empirical, but useful, tool to try forecasting the maximum expected erupted volumes of paroxysms or the repose time, helping the evaluation of volcanic hazards (Bonaccorso & Calvari, 2013; Calvari et al., 2020; Calvari & Nunnari, 2022). For this reason, it is important to identify, study, and understand the steady state activity in volcanoes and magmatic provinces worldwide. Our data also confirm the fact that after many decades, the steady state regime can suddenly shift to different steady state rates, starting a new episode. The investigation of how the steady state rate, as well as how the changes in the steady state rates between

episodes, relate to the longer-term rates might further improve the understanding of the volcanic activity and should be pursued in future studies, despite the difficulty in constraining the eruptive rates on long time scales.

Acknowledgments:

F. Galetto and M. E. Pritchard were supported by NASA Grant 80NSSC20K1674 from the Interdisciplinary Science Program of the Earth Science Division.

We are grateful to the Editor Magdalena Oryaëlle Chevrel for the helpful comments and suggestions and for the assistance in the editorial process, and to Matt Patrick and other two anonymous reviewers for their helpful comments and suggestions that improved the quality of this manuscript.

Data availability statement:

Codes for the *Q-line fitting* method and the *deterministic time interval* method, as well as the dataset used in Figures 7-8, have been uploaded in a public repository and are available at https://github.com/basfora/ssvolcanism

Datasets reported in Figures 3-6 are reported in Supplementary Tables S1-S4. All the Supplementary files (Supplementary Tables S1-S6, Supplementary Text S1-S4, Supplementary Figures S1-S8) have been uploaded also in a permanent data repository and are available at https://doi.org/10.17605/OSF.IO/HR4XT. Data in Figures 3-6 come from the following references, also reported in Tables S1-S4:

(Aubry et al., 2021; Bagnardi et al., 2013; Bagnardi & Amelung, 2012; Bernard et al., 2019; Blasizzo et al., 2022; Campus et al., 2025; Caracciolo et al., 2024; Chadwick et al., 1991, 2011; Chevrel et al., 2022, 2023; Davis et al., 2021; De Novellis et al., 2017; Derrien, 2019; Dietterich et al., 2021; Dumont et al., 2022; Dvorak & Dzurisin, 1993; Dzurisin et al., 1984; Galetto, 2023; Galetto et al., 2019, 2020, 2024, 2025; Galetto, Reale, et al., 2023; Geist et al., 2008; Global Volcanism Program, 2025; Gudmundsson et al., 1997, 2012, 2016; Gudmundsson & Björnsson, 1991; Guo et al., 2019; Harris et al., 2000; Heliker & Mattox, 2003; Howard et al., 2019; Hreinsdóttir et al., 2014; Hrysiewicz et al., 2025; Jónsson et al., 1999; Jude-Eton et al., 2012; Kauahikaua & Trusdell, 2020; Lockwood & Lipman, 1987; Macdonald et al., 1983; Macdonald & Hubbard, 1961; Mulliken et al., 2024; Naumann et al., 2002; Naumann & Geist, 2000; Neal et al., 2019; Orr et al., 2015; OVPF-IPG, 2021; Parks et al., 2023, 2025; Pedersen et al., 2018, 2022, 2024; Peltier et al., 2009, 2018, 2020; Reddin et al., 2024; Roult et al., 2012; Rowland, 1996; Rowland et al., 2003; Schipper et al., 2015; Shreve & Delgado,

2023; Staudacher et al., 2016; Stearns & Macdonald, 1946; Sturkell et al., 2003; Sutton et al., 2003; Swanson, 1972; Teasdale et al., 2005; Thorarinsson & Sigvaldason, 1962; Thordarson & Sigmarsson, 2009; Tryggvason, 1984, 1986; Vasconez et al., 2018; Williams Jr. & Moore, 1976; Wolfe et al., 1987; Wright & Klein, 2014; Xu et al., 2016, 2023).

Further references in the supplementary text S1-S4, which are not reported in the main text or in the Supplementary Tables S1-S4:

(Eiden et al., 2023; Farr et al., 2007; Krieger et al., 2007, 2013; Kubanek et al., 2017)

635 **References**

636 Aubry, T. J., Engwell, S., Bonadonna, C., Carazzo, G., Scollo, S., Van Eaton, A. R., Taylor, I. A.,
637 Jessop, D., Eychenne, J., Gouhier, M., Mastin, L. G., Wallace, K. L., Biass, S., Bursik, M.,
638 Grainger, R. G., Jellinek, A. M., & Schmidt, A. (2021). The Independent Volcanic Eruption
639 Source Parameter Archive (IVESPA, version 1.0): A new observational database to support
640 explosive eruptive column model validation and development. *Journal of Volcanology and*
641 *Geothermal Research*, *417*, 107295. https://doi.org/10.1016/j.jvolgeores.2021.107295

642 Bablon, M., Quidelleur, X., Samaniego, P., Le Pennec, J.-L., Santamaría, S., Liorzou, C., Hidalgo,
643 S., & Eschbach, B. (2020). Volcanic history reconstruction in northern Ecuador: Insights for
644 eruptive and erosion rates on the whole Ecuadorian arc. *Bulletin of Volcanology*, *82*(1), 11.
645 https://doi.org/10.1007/s00445-019-1346-1

646 Bagnardi, M., & Amelung, F. (2012). Space-geodetic evidence for multiple magma reservoirs and
647 subvolcanic lateral intrusions at Fernandina Volcano, Galápagos Islands. *Journal of*
648 *Geophysical Research: Solid Earth*, *117*(B10). https://doi.org/10.1029/2012JB009465

649 Bagnardi, M., Amelung, F., & Poland, M. P. (2013). A new model for the growth of basaltic shields
650 based on deformation of Fernandina volcano, Galápagos Islands. *Earth and Planetary Science*
651 *Letters*, *377–378*, 358–366. https://doi.org/10.1016/j.epsl.2013.07.016

652 Bagnardi, M., González, P. J., & Hooper, A. (2016). High-resolution digital elevation model from tri-
653 stereo Pleiades-1 satellite imagery for lava flow volume estimates at Fogo Volcano.
654 *Geophysical Research Letters*, *43*(12), 6267–6275. https://doi.org/10.1002/2016GL069457

655 Bebbington, M. S. (2014). Long-term forecasting of volcanic explosivity. *Geophysical Journal*
656 *International*, *197*(3), 1500–1515. https://doi.org/10.1093/gji/ggu078

657 Bernard, B., Stock, M. J., Coppola, D., Hidalgo, S., Bagnardi, M., Gibson, S., Hernandez, S., Ramón,
658 P., & Gleeson, M. (2019). Chronology and phenomenology of the 1982 and 2015 Wolf
659 volcano eruptions, Galápagos Archipelago. *Journal of Volcanology and Geothermal*
660 *Research*, *374*, 26–38. https://doi.org/10.1016/j.jvolgeores.2019.02.013

661 Blasizzo, A. Y., Ukstins, I. A., Scheidt, S. P., Graettinger, A. H., Peate, D. W., Carley, T. L., Moritz,
662 A. J., & Thines, J. E. (2022). Vikrahraun—the 1961 basaltic lava flow eruption at Askja,
663 Iceland: Morphology, geochemistry, and planetary analogs. *Earth, Planets and Space*, *74*(1),
664 168. https://doi.org/10.1186/s40623-022-01711-5
665 Bonaccorso, A., & Calvari, S. (2013). Major effusive eruptions and recent lava fountains: Balance
666 between expected and erupted magma volumes at Etna volcano. *Geophysical Research*
667 *Letters*, *40*(23), 6069–6073. https://doi.org/10.1002/2013GL058291
668 Burgi, P.-Y., Valade, S., Coppola, D., Boudoire, G., Mavonga, G., Rufino, F., & Tedesco, D. (2021).
669 Unconventional filling dynamics of a pit crater. *Earth and Planetary Science Letters*, *576*,
670 117230. https://doi.org/10.1016/j.epsl.2021.117230
671 Calvari, S., Bilotta, G., Bonaccorso, A., Caltabiano, T., Cappello, A., Corradino, C., Del Negro, C.,
672 Ganci, G., Neri, M., Pecora, E., Salerno, G. G., & Spampinato, L. (2020). The VEI 2
673 Christmas 2018 Etna Eruption: A Small But Intense Eruptive Event or the Starting Phase of
674 a Larger One? *Remote Sensing*, *12*(6), Articolo 6. https://doi.org/10.3390/rs12060905
675 Calvari, S., & Nunnari, G. (2022). Etna Output Rate during the Last Decade (2011–2022): Insights
676 for Hazard Assessment. *Remote Sensing*, *14*(23), Articolo 23.
677 https://doi.org/10.3390/rs14236183
678 Campus, A., Villeneuve, N., Chevrel, O., Peltier, A., Di Muro, A., & Coppola, D. (2025). Effusion
679 Rate Trends at Piton de la Fournaise: A Review of 24 Years of Space-Based Thermal
680 Observation. *Journal of Geophysical Research: Solid Earth*, *130*(6), e2024JB030962.
681 https://doi.org/10.1029/2024JB030962
682 Cappello, A., Ganci, G., Bilotta, G., Corradino, C., Hérault, A., & Del Negro, C. (2019). Changing
683 Eruptive Styles at the South-East Crater of Mount Etna: Implications for Assessing Lava Flow
684 Hazards. *Frontiers in Earth Science*, *7*. https://doi.org/10.3389/feart.2019.00213

685 Caracciolo, A., Bali, E., Ranta, E., Guðfinnsson, G. H., & Óskarsson, B. V. (2024). Medieval and
686 recent SO2 budgets in the Reykjanes Peninsula: Implication for future hazard. *Geochemical*
687 *Perspectives Letters*, *30*, 20–27. https://doi.org/10.7185/geochemlet.2417
688 Chadwick, W. W., De Roy, T., & Carrasco, A. (1991). The September 1988 intracaldera avalanche
689 and eruption at Fernandina volcano, Galapagos Islands. *Bulletin of Volcanology*, *53*(4), 276–
690 286. https://doi.org/10.1007/BF00414524
691 Chadwick, W. W., Jónsson, S., Geist, D. J., Poland, M., Johnson, D. J., Batt, S., Harpp, K. S., & Ruiz,
692 A. (2011). The May 2005 eruption of Fernandina volcano, Galápagos: The first
693 circumferential dike intrusion observed by GPS and InSAR. *Bulletin of Volcanology*, *73*(6),
694 679–697. https://doi.org/10.1007/s00445-010-0433-0
695 Chevrel, M. O., Harris, A., Peltier, A., Villeneuve, N., Coppola, D., Gouhier, M., & Drenne, S.
696 (2022). Volcanic crisis management supported by near real-time lava flow hazard assessment
697 at Piton de la Fournaise, La Réunion. *Volcanica*, *5*(2), 313–334.
698 https://doi.org/10.30909/vol.05.02.313334
699 Chevrel, M. O., Villeneuve, N., Grandin, R., Froger, J.-L., Coppola, D., Massimetti, F., Campus, A.,
700 Hrysiewicz, A., & Peltier, A. (2023). Lava flow daily monitoring: The case of the 19
701 September–5 October 2022 eruption at Piton de la Fournaise. *Volcanica*, *6*(2), 391–404.
702 https://doi.org/10.30909/vol.06.02.391404
703 Civetta, L., Cornette, Y., Gillot, P. Y., & Orsi, G. (1988). The eruptive history of Pantelleria (Sicily
704 channel) in the last 50 ka. *Bulletin of Volcanology*, *50*(1), 47–57.
705 https://doi.org/10.1007/BF01047508
706 Clocchiatti, R., Condomines, M., Guénot, N., & Tanguy, J.-C. (2004). Magma changes at Mount
707 Etna: The 2001 and 2002–2003 eruptions. *Earth and Planetary Science Letters*, *226*(3), 397–
708 414. https://doi.org/10.1016/j.epsl.2004.07.039
709 Coppola, D., Laiolo, M., Franchi, A., Massimetti, F., Cigolini, C., & Lara, L. E. (2017). Measuring
710 effusion rates of obsidian lava flows by means of satellite thermal data. *Journal of*

711 *Volcanology and Geothermal Research*, *347*, 82–90.
712 https://doi.org/10.1016/j.jvolgeores.2017.09.003
713 Coppola, D., Laiolo, M., Massimetti, F., Hainzl, S., Shevchenko, A. V., Mania, R., Shapiro, N. M.,
714 & Walter, T. R. (2021). Thermal remote sensing reveals communication between volcanoes
715 of the Klyuchevskoy Volcanic Group. *Scientific Reports*, *11*(1), 13090.
716 https://doi.org/10.1038/s41598-021-92542-z
717 Coppola, D., Piscopo, D., Staudacher, T., & Cigolini, C. (2009). Lava discharge rate and effusive
718 pattern at Piton de la Fournaise from MODIS data. *Journal of Volcanology and Geothermal*
719 *Research, Recent advances on the geodynamics of Piton de la Fournaise volcano*, *184*(1),
720 174–192. https://doi.org/10.1016/j.jvolgeores.2008.11.031
721 Coppola, D., Valade, S., Masias, P., Laiolo, M., Massimetti, F., Campus, A., Aguilar, R., Anccasi,
722 R., Apaza, F., Ccallata, B., Cigolini, C., Cruz, L. F., Finizola, A., Gonzales, K., Macedo, O.,
723 Miranda, R., Ortega, M., Paxi, R., Taipe, E., & Valdivia, D. (2022). Shallow magma
724 convection evidenced by excess degassing and thermal radiation during the dome-forming
725 Sabancaya eruption (2012–2020). *Bulletin of Volcanology*, *84*(2), 16.
726 https://doi.org/10.1007/s00445-022-01523-1
727 Crisp, J. A. (1984). Rates of magma emplacement and volcanic output. *Journal of Volcanology and*
728 *Geothermal Research*, *20*(3), 177–211. https://doi.org/10.1016/0377-0273(84)90039-8
729 Dai, C., & Howat, I. M. (2017). Measuring Lava Flows With ArcticDEM: Application to the 2012–
730 2013 Eruption of Tolbachik, Kamchatka. *Geophysical Research Letters*, *44*(24), 12,133-
731 12,140. https://doi.org/10.1002/2017GL075920
732 Davis, T., Bagnardi, M., Lundgren, P., & Rivalta, E. (2021). Extreme Curvature of Shallow Magma
733 Pathways Controlled by Competing Stresses: Insights From the 2018 Sierra Negra Eruption.
734 *Geophysical Research Letters*, *48*(13), e2021GL093038.
735 https://doi.org/10.1029/2021GL093038

De Beni, E., Cantarero, M., Neri, M., & Messina, A. (2021). Lava flows of Mt Etna, Italy: The 2019 eruption within the context of the last two decades (1999–2019). *Journal of Maps*, *17*(3), 65–76. https://doi.org/10.1080/17445647.2020.1854131

De la Cruz-Reyna, S. (1991). Poisson-distributed patterns of explosive eruptive activity. *Bulletin of Volcanology*, *54*(1), 57–67. https://doi.org/10.1007/BF00278206

De Novellis, V., Castaldo, R., De Luca, C., Pepe, S., Zinno, I., Casu, F., Lanari, R., & Solaro, G. (2017). Source modelling of the 2015 Wolf volcano (Galápagos) eruption inferred from Sentinel 1-A DInSAR deformation maps and pre-eruptive ENVISAT time series. *Journal of Volcanology and Geothermal Research, Volcano Geodesy: Recent developments and future challenges*, *344*, 246–256. https://doi.org/10.1016/j.jvolgeores.2017.05.013

Derrien, A. (2019). *Apports des techniques photogrammétriques à l'étude du dynamisme des structures volcaniques du piton de la Fournaise* [PhD Thesis]. http://www.theses.fr/2019UNIP7084/document

Di Renzo, V., Corsaro, R. A., Miraglia, L., Pompilio, M., & Civetta, L. (2019). Long and short-term magma differentiation at Mt. Etna as revealed by Sr-Nd isotopes and geochemical data. *Earth-Science Reviews*, *190*, 112–130. https://doi.org/10.1016/j.earscirev.2018.12.008

Dietterich, H. R., Diefenbach, A. K., Soule, S. A., Zoeller, M. H., Patrick, M. P., Major, J. J., & Lundgren, P. R. (2021). Lava effusion rate evolution and erupted volume during the 2018 Kīlauea lower East Rift Zone eruption. *Bulletin of Volcanology*, *83*(4), 25. https://doi.org/10.1007/s00445-021-01443-6

Dumont, Q., Cayol, V., Froger, J.-L., & Peltier, A. (2022). 22 years of satellite imagery reveal a major destabilization structure at Piton de la Fournaise. *Nature Communications*, *13*(1), 2649. https://doi.org/10.1038/s41467-022-30109-w

Dvorak, J. J., & Dzurisin, D. (1993). Variations in magma supply rate at Kilauea Volcano, Hawaii. *Journal of Geophysical Research: Solid Earth*, *98*(B12), 22255–22268. https://doi.org/10.1029/93JB02765

762 Dzurisin, D., Koyanagi, R. Y., & English, T. T. (1984). Magma supply and storage at Kilauea
763 volcano, Hawaii, 1956–1983. *Journal of Volcanology and Geothermal Research*, *21*(3), 177–
764 206. https://doi.org/10.1016/0377-0273(84)90022-2
765 Eiden, E., Pritchard, M. E., & Lundgren, P. R. (2023). Spatial and Temporal Resolution Needs for
766 Volcano Topographic Change Data Sets Based on Past Eruptions (1980–2019). *Earth and*
767 *Space Science*, *10*(10), e2023EA003054. https://doi.org/10.1029/2023EA003054
768 Farr, T. G., Rosen, P. A., Caro, E., Crippen, R., Duren, R., Hensley, S., Kobrick, M., Paller, M.,
769 Rodriguez, E., Roth, L., Seal, D., Shaffer, S., Shimada, J., Umland, J., Werner, M., Oskin, M.,
770 Burbank, D., & Alsdorf, D. (2007). The Shuttle Radar Topography Mission. *Reviews of*
771 *Geophysics*, *45*(2). https://doi.org/10.1029/2005RG000183
772 Galetto, F. (2023). Complex paths of magma propagation at Fernandina (Galápagos): The coexistence
773 of circumferential and radial dike intrusion during the January 2020 eruption. *Bulletin of*
774 *Volcanology*, *85*(12), 71. https://doi.org/10.1007/s00445-023-01688-3
775 Galetto, F., Bagnardi, M., Acocella, V., & Hooper, A. (2019). Noneruptive Unrest at the Caldera of
776 Alcedo Volcano (Galápagos Islands) Revealed by InSAR Data and Geodetic Modeling.
777 *Journal of Geophysical Research: Solid Earth*, *124*(4), 3365–3381.
778 https://doi.org/10.1029/2018JB017103
779 Galetto, F., Dualeh, E., Delgado, F., Pritchard, M., Poland, M., Ebmeier, S., Shreve, T., Biggs, J.,
780 Hamling, I., Wauthier, C., Santana, J. G., Froger, J.-L., & Bemelmans, M. (2024). The utility
781 of TerraSAR-X, TanDEM-X, and PAZ for studying global volcanic activity: Successes,
782 challenges, and future prospects. *Volcanica*, *7*(1), Articolo 1.
783 https://doi.org/10.30909/vol.07.01.273301
784 Galetto, F., Hooper, A., Bagnardi, M., & Acocella, V. (2020). The 2008 Eruptive Unrest at Cerro
785 Azul Volcano (Galápagos) Revealed by InSAR Data and a Novel Method for Geodetic
786 Modelling. *Journal of Geophysical Research: Solid Earth*, *125*(2), e2019JB018521.
787 https://doi.org/10.1029/2019JB018521

788 Galetto, F., Miller, S. M., Barris, R., Shevchenko, A. V., & Pritchard, M. E. (2025). The application
789 of high resolution EarthDEM and ArcticDEM digital elevation models to detect and quantify
790 volcanic activity: Successes and challenges. *Bulletin of Volcanology*, *87*(7), 53.
791 https://doi.org/10.1007/s00445-025-01838-9
792 Galetto, F., Pritchard, M. E., Hornby, A. J., Gazel, E., & Mahowald, N. M. (2023). Spatial and
793 Temporal Quantification of Subaerial Volcanism From 1980 to 2019: Solid Products, Masses,
794 and Average Eruptive Rates. *Reviews of Geophysics*, *61*(1), e2022RG000783.
795 https://doi.org/10.1029/2022RG000783
796 Galetto, F., Reale, D., Sansosti, E., & Acocella, V. (2023). Implications for Shallow Magma Transfer
797 During the 2017 and 2018 Eruptions at Fernandina (Galápagos) Inferred From InSAR Data.
798 *Journal of Geophysical Research: Solid Earth*, *128*(6), e2022JB026174.
799 https://doi.org/10.1029/2022JB026174
800 Geist, D. J. (1996). On the emergence and submergence of the Galápagos Islands. *Noticias de*
801 *Galápagos*, *56*, 5–9.
802 Geist, D. J., Bergantz, G., & Chadwick Jr., W. W. (2014). Galápagos Magma Chambers. In *The*
803 *Galápagos* (pp. 55–69). American Geophysical Union (AGU).
804 https://doi.org/10.1002/9781118852538.ch5
805 Geist, D. J., Harpp, K. S., Naumann, T. R., Poland, M., Chadwick, W. W., Hall, M., & Rader, E.
806 (2008). The 2005 eruption of Sierra Negra volcano, Galápagos, Ecuador. *Bulletin of*
807 *Volcanology*, *70*(6), 655–673. https://doi.org/10.1007/s00445-007-0160-3
808 Geist, D. J., Howard, K. A., Jellinek, A. M., & Rayder, S. (1994). The volcanic history of Volcán
809 Alcedo, Galápagos Archipelago: A case study of rhyolitic oceanic volcanism. *Bulletin of*
810 *Volcanology*, *56*(4), 243–260. https://doi.org/10.1007/BF00302078
811 Geist, D. J., Naumann, T., Standish, J. J., Kurz, M. D., Harpp, K. S., White, W. M., & Fornari, D. J.
812 (2005). Wolf Volcano, Galápagos Archipelago: Melting and Magmatic Evolution at the

Margins of a Mantle Plume. *Journal of Petrology*, *46*(11), 2197–2224. https://doi.org/10.1093/petrology/egi052

Gerlach, D. C. (1990). Eruption rates and isotopic systematics of ocean islands: Further evidence for small-scale heterogeneity in the upper mantle. *Tectonophysics*, *172*(3), 273–289. https://doi.org/10.1016/0040-1951(90)90035-7

Global Volcanism Program. (2025). *Volcanoes of the World (v. 5.3.3; 26 Nov 2025).* [Database]. Distributed by Smithsonian Institution, compiled by Venzke, E. https://doi.org/10.5479/si.GVP.VOTW5-2025.5.3

Greene, A. R., Garcia, M. O., Pietruszka, A. J., Weis, D., Marske, J. P., Vollinger, M. J., & Eiler, J. (2013). Temporal geochemical variations in lavas from Kīlauea's Pu'u 'Ō'ō eruption (1983–2010): Cyclic variations from melting of source heterogeneities. *Geochemistry, Geophysics, Geosystems*, *14*(11), 4849–4873. https://doi.org/10.1002/ggge.20285

Gudmundsson, M. T., & Björnsson, H. (1991). Eruptions in Grímsvötn, Vatnajökull, Iceland, 1934-1991. *Eruptions in Grímsvötn, Vatnajökull, Iceland, 1934-1991*, (41), 21–45. https://doi.org/10.33799/jokull1991.41.021

Gudmundsson, M. T., Jónsdóttir, K., Hooper, A., Holohan, E. P., Halldórsson, S. A., Ófeigsson, B. G., Cesca, S., Vogfjörd, K. S., Sigmundsson, F., Högnadóttir, T., Einarsson, P., Sigmarsson, O., Jarosch, A. H., Jónasson, K., Magnússon, E., Hreinsdóttir, S., Bagnardi, M., Parks, M. M., Hjörleifsdóttir, V., … Aiuppa, A. (2016). Gradual caldera collapse at Bárdarbunga volcano, Iceland, regulated by lateral magma outflow. *Science*, *353*(6296), aaf8988. https://doi.org/10.1126/science.aaf8988

Gudmundsson, M. T., Sigmundsson, F., & Björnsson, H. (1997). Ice–volcano interaction of the 1996 Gjálp subglacial eruption, Vatnajökull, Iceland. *Nature*, *389*(6654), 954–957. https://doi.org/10.1038/40122

Gudmundsson, M. T., Thordarson, T., Höskuldsson, Á., Larsen, G., Björnsson, H., Prata, F. J., Oddsson, B., Magnússon, E., Högnadóttir, T., Petersen, G. N., Hayward, C. L., Stevenson, J.

A., & Jónsdóttir, I. (2012). Ash generation and distribution from the April-May 2010 eruption of Eyjafjallajökull, Iceland. *Scientific Reports*, *2*(1), 572. https://doi.org/10.1038/srep00572

Guo, Q., Xu, C., Wen, Y., Liu, Y., & Xu, G. (2019). The 2017 Noneruptive Unrest at the Caldera of Cerro Azul Volcano (Galápagos Islands) Revealed by InSAR Observations and Geodetic Modelling. *Remote Sensing*, *11*(17), Articolo 17. https://doi.org/10.3390/rs11171992

Harpp, K. S., & Geist, D. J. (2018). The Evolution of Galápagos Volcanoes: An Alternative Perspective. *Frontiers in Earth Science*, *6*. https://doi.org/10.3389/feart.2018.00050

Harris, A. J. L., Dehn, J., & Calvari, S. (2007). Lava effusion rate definition and measurement: A review. *Bulletin of Volcanology*, *70*(1), 1–22. https://doi.org/10.1007/s00445-007-0120-y

Harris, A. J. L., Murray, J. B., Aries, S. E., Davies, M. A., Flynn, L. P., Wooster, M. J., Wright, R., & Rothery, D. A. (2000). Effusion rate trends at Etna and Krafla and their implications for eruptive mechanisms. *Journal of Volcanology and Geothermal Research*, *102*(3), 237–269. https://doi.org/10.1016/S0377-0273(00)00190-6

Harris, A., Steffke, A., Calvari, S., & Spampinato, L. (2011). Thirty years of satellite-derived lava discharge rates at Etna: Implications for steady volumetric output. *Journal of Geophysical Research: Solid Earth*, *116*(B8). https://doi.org/10.1029/2011JB008237

Heliker, C., & Mattox, T. N. (2003). The First Two Decades of the Pu‘u ‘Õ‘ō-Kūpaianaha Eruption: Chronology and Selected Bibliography. *US Geological Survey Professional Paper*, *1676*, 1.

Howard, K. A., Simkin, T., Geist, D. J., Merlen, G., & Nolf, B. (2019). Large hydromagmatic eruption related to Fernandina Volcano’s 1968 caldera collapse—Deposits, landforms, and ecosystem recovery. In M. P. Poland, M. O. Garcia, V. E. Camp, & A. Grunder (A c. Di), *Field Volcanology: A Tribute to the Distinguished Career of Don Swanson* (Vol. 538, p. 0). Geological Society of America. https://doi.org/10.1130/2018.2538(18)

Hreinsdóttir, S., Sigmundsson, F., Roberts, M. J., Björnsson, H., Grapenthin, R., Arason, P., Árnadóttir, T., Hólmjárn, J., Geirsson, H., Bennett, R. A., Gudmundsson, M. T., Oddsson, B., Ófeigsson, B. G., Villemin, T., Jónsson, T., Sturkell, E., Höskuldsson, Á., Larsen, G.,

865 Thordarson, T., & Óladóttir, B. A. (2014). Volcanic plume height correlated with magma-
866 pressure change at Grímsvötn Volcano, Iceland. *Nature Geoscience*, *7*(3), 214–218.
867 https://doi.org/10.1038/ngeo2044
868 Hrysiewicz, A., LaFemina, P. C., Bell, A., Galetto, F., Vallejo, S., Bernard, B., & Holohan, E. P.
869 (2025). Lava Tube System Development Defined by Multispectral Imaging and InSAR: The
870 Case of the 2024 Eruption of Fernandina Volcano (Galápagos). *Journal of Geophysical*
871 *Research: Solid Earth*, *130*(11), e2025JB032265. https://doi.org/10.1029/2025JB032265
872 Jicha, B. R., & Singer, B. S. (2006). Volcanic history and magmatic evolution of Seguam Island,
873 Aleutian Island arc, Alaska. *GSA Bulletin*, *118*(7–8), 805–822.
874 https://doi.org/10.1130/B25861.1
875 Jónsson, S., Zebker, H., Cervelli, P., Segall, P., Garbeil, H., Mouginis-Mark, P., & Rowland, S.
876 (1999). A shallow-dipping dike fed the 1995 flank eruption at Fernandina Volcano,
877 Galápagos, observed by satellite radar interferometry. *Geophysical Research Letters*, *26*(8),
878 1077–1080. https://doi.org/10.1029/1999GL900108
879 Jude-Eton, T. C., Thordarson, T., Gudmundsson, M. T., & Oddsson, B. (2012). Dynamics,
880 stratigraphy and proximal dispersal of supraglacial tephra during the ice-confined 2004
881 eruption at Grímsvötn Volcano, Iceland. *Bulletin of Volcanology*, *74*(5), 1057–1082.
882 https://doi.org/10.1007/s00445-012-0583-3
883 Kauahikaua, J., & Trusdell, F. A. (2020). *Have humans influenced volcanic activity on the lower East*
884 *Rift Zone of Kīlauea Volcano? A publication review* (Report Nos. 2020–1017; Open-File
885 Report, p. 17). USGS Publications Warehouse. https://doi.org/10.3133/ofr20201017
886 King, C.-Y. (1989). Volume predictability of historical eruptions at Kilauea and Mauna Loa
887 volcanoes. *Journal of Volcanology and Geothermal Research*, *38*(3), 281–285.
888 https://doi.org/10.1016/0377-0273(89)90043-7
889 Klein, F. W., Koyanagi, R. Y., Nakata, J. S., & Tanigawa, W. R. (1987). The seismicity of Kilauea's
890 magma system. *Volcanism in Hawaii*, *2*, 1019–1185.

Krieger, G., Moreira, A., Fiedler, H., Hajnsek, I., Werner, M., Younis, M., & Zink, M. (2007). TanDEM-X: A Satellite Formation for High-Resolution SAR Interferometry. *IEEE Transactions on Geoscience and Remote Sensing*, *45*(11), 3317–3341. https://doi.org/10.1109/TGRS.2007.900693

Krieger, G., Zink, M., Bachmann, M., Bräutigam, B., Breit, H., Fiedler, H., Fritz, T., Hajnsek, I., Gonzalez, J. H., Kahle, R., König, R., Schättler, B., Schulze, D., Ulrich, D., Wermuth, M., Wessel, B., & Moreira, A. (2013). TanDEM-X. In M. D'Errico (A c. Di), *Distributed Space Missions for Earth System Monitoring* (pp. 387–435). Springer. https://doi.org/10.1007/978-1-4614-4541-8_13

Kubanek, J., Westerhaus, M., & Heck, B. (2017). TanDEM-X Time Series Analysis Reveals Lava Flow Volume and Effusion Rates of the 2012–2013 Tolbachik, Kamchatka Fissure Eruption. *Journal of Geophysical Research: Solid Earth*, *122*(10), 7754–7774. https://doi.org/10.1002/2017JB014309

Kubanek, J., Westerhaus, M., Schenk, A., Aisyah, N., Brotopuspito, K. S., & Heck, B. (2015). Volumetric change quantification of the 2010 Merapi eruption using TanDEM-X InSAR. *Remote Sensing of Environment*, *164*, 16–25. https://doi.org/10.1016/j.rse.2015.02.027

Kuntz, M. A., Champion, D. E., Spiker, E. C., & Lefebvre, R. H. (1986). Contrasting magma types and steady-state, volume-predictable, basaltic volcanism along the Great Rift, Idaho. *GSA Bulletin*, *97*(5), 579–594. https://doi.org/10.1130/0016-7606(1986)97%253C579:CMTASV%253E2.0.CO;2

Kurz, M. D., Rowland, S. K., Curtice, J., Saal, A. E., & Naumann, T. (2014). Eruption Rates for Fernandina Volcano. In *The Galápagos* (pp. 41–54). American Geophysical Union (AGU). https://doi.org/10.1002/9781118852538.ch4

Lipman, P. W. (1995). Declining growth of Mauna Loa during the last 100,000 years: Rates of lava accumulation vs. Gravitational subsidence. *Mauna Loa revealed: structure, composition, history, and hazards*, *92*, 45–80.

Lipman, P. W. (2000). Central San Juan caldera cluster: Regional volcanic framework. *GSA Special Papers*, *346*, 9–69. https://doi.org/10.1130/0-8137-2346-9.9

Lockwood, J. P., & Lipman, P. W. (1987). *Holocene eruptive history of Mauna Loa volcano*. *1350*.

Macdonald, G. A., Abbott, A., & Peterson, F. L. (1983). *Volcanoes in the sea: The geology of Hawaii (2nd ed.)*. University of Hawaii press.

Macdonald, G. A., & Hubbard, D. H. (1961). *Volcanoes of the National Parks in Hawaii*. Hawaii Natural History Association.

Marturano, A., Isaia, R., Aiello, G., & Barra, D. (2018). Complex Dome Growth at Campi Flegrei Caldera (Italy) in the Last 15 ka. *Journal of Geophysical Research: Solid Earth*, *123*(9), 8180–8197. https://doi.org/10.1029/2018JB015672

Montgomery-Brown, E. K., & Miklius, A. (2020). Periodic dike intrusions at Kīlauea volcano, Hawai'i. *Geology*, *49*(4), 397–401. https://doi.org/10.1130/G47970.1

Moore, J. G. (1970). Relationship between subsidence and volcanic load, Hawaii. *Bulletin Volcanologique*, *34*(2), 562–576.

Mulliken, K. M., Kauahikaua, J. P., Swanson, D., & Zoeller, M. H. (2024). Chronology of recent volcanic activity on the Island of Hawai'i, Hawaii. *US Geological Survey (USGS) Data Release*, 76.

Nasholds, M. W. M., & Zimmerer, M. J. (2022). High-precision 40Ar/39Ar geochronology and volumetric investigation of volcanism and resurgence following eruption of the Tshirege Member, Bandelier Tuff, at the Valles caldera. *Journal of Volcanology and Geothermal Research*, *431*, 107624. https://doi.org/10.1016/j.jvolgeores.2022.107624

Naumann, T., & Geist, D. J. (2000). Physical volcanology and structural development of Cerro Azul Volcano, Isabela Island, Galápagos: Implications for the development of Galápagos-type shield volcanoes. *Bulletin of Volcanology*, *61*(8), 497–514. https://doi.org/10.1007/s004450050001

942 Naumann, T., Geist, D. J., & Kurz, M. (2002). Petrology and Geochemistry of Volcán Cerro Azul:
943 Petrologic Diversity among the Western Galápagos Volcanoes. *Journal of Petrology*, *43*(5),
944 859–883. https://doi.org/10.1093/petrology/43.5.859
945 Neal, C. A., Brantley, S. R., Antolik, L., Babb, J. L., Burgess, M., Calles, K., Cappos, M., Chang, J.
946 C., Conway, S., Desmither, L., Dotray, P., Elias, T., Fukunaga, P., Fuke, S., Johanson, I. A.,
947 Kamibayashi, K., Kauahikaua, J., Lee, R. L., Pekalib, S., … Damby, D. (2019). The 2018 rift
948 eruption and summit collapse of Kīlauea Volcano. *Science*, *363*(6425), 367–374.
949 https://doi.org/10.1126/science.aav7046
950 O'Hagan, A., & Leonard, T. (1976). Bayes estimation subject to uncertainty about parameter
951 constraints. *Biometrika*, *63*(1), 201–203. https://doi.org/10.1093/biomet/63.1.201
952 Orr, T. R., Poland, M. P., Patrick, M. R., Thelen, W. A., Sutton, A. J., Elias, T., Thornber, C. R.,
953 Parcheta, C., & Wooten, K. M. (2015). Kīlauea's 5–9 March 2011 Kamoamoa Fissure
954 Eruption and Its Relation to 30+ Years of Activity From Pu'u 'Ō 'ō. In *Hawaiian Volcanoes*
955 (pp. 393–420). https://doi.org/10.1002/9781118872079.ch18
956 OVPF-IPG. (2021). *Rapport Annuel 2021*. Observatoire Volcanologique du Piton de la Fournaise -
957 Institut de Physique du Globe de Paris. ISSN 2610-5101.
958 https://www.ipgp.fr/en/observation/ovs/ovpf/ovpf-ipgp-annual-activity-reports/
959 Parks, M., Drouin, V., Sigmundsson, F., Hjartardóttir, Á. R., Geirsson, H., Pedersen, G. B. M., Belart,
960 J. M. C., Barsotti, S., Lanzi, C., Vogfjörd, K., Hooper, A., Ófeigsson, B., Hreinsdóttir, S.,
961 Gestsson, E. B., Þrastarson, R. H., Einarsson, P., Tolpekin, V., Rotheram-Clarke, D.,
962 Gunnarsson, S. R., … Pinel, V. (2025). 2023–2024 inflation-deflation cycles at Svartsengi
963 and repeated dike injections and eruptions at the Sundhnúkur crater row, Reykjanes Peninsula,
964 Iceland. *Earth and Planetary Science Letters*, *658*, 119324.
965 https://doi.org/10.1016/j.epsl.2025.119324
966 Parks, M., Sigmundsson, F., Drouin, V., Hjartardóttir, Á. R., Geirsson, H., Hooper, A., Vogfjörd, K.
967 S., Ófeigsson, B. G., Hreinsdóttir, S., Jensen, E. H., Einarsson, P., Barsotti, S., &

968 Fridriksdóttir, H. M. (2023). Deformation, seismicity, and monitoring response preceding and
969 during the 2022 Fagradalsfjall eruption, Iceland. *Bulletin of Volcanology*, *85*(10), 60.
970 https://doi.org/10.1007/s00445-023-01671-y
971 Pedersen, G. B. M., Belart, J. M. C., Magnússon, E., Vilmundardóttir, O. K., Kizel, F.,
972 Sigurmundsson, F. S., Gísladóttir, G., & Benediktsson, J. A. (2018). Hekla Volcano, Iceland,
973 in the 20th Century: Lava Volumes, Production Rates, and Effusion Rates. *Geophysical*
974 *Research Letters*, *45*(4), 1805–1813. https://doi.org/10.1002/2017GL076887
975 Pedersen, G. B. M., Belart, J. M. C., Óskarsson, B. V., Gudmundsson, M. T., Gies, N., Högnadóttir,
976 T., Hjartardóttir, Á. R., Pinel, V., Berthier, E., Dürig, T., Reynolds, H. I., Hamilton, C. W.,
977 Valsson, G., Einarsson, P., Ben-Yehosua, D., Gunnarsson, A., & Oddsson, B. (2022).
978 Volume, Effusion Rate, and Lava Transport During the 2021 Fagradalsfjall Eruption: Results
979 From Near Real-Time Photogrammetric Monitoring. *Geophysical Research Letters*, *49*(13),
980 e2021GL097125. https://doi.org/10.1029/2021GL097125
981 Pedersen, G. B. M., Belart, J. M. C., Óskarsson, B. V., Gunnarson, S. R., Gudmundsson, M. T.,
982 Reynolds, H. I., Valsson, G., Högnadóttir, Thórdís., Pinel, V., Parks, M. M., Drouin, V.,
983 Askew, R. A., Dürig, T., & Drastarson, R. H. (2024). *Volume, effusion rates and lava hazards*
984 *of the 2021, 2022 and 2023 Reykjanes fires: Lessons learned from near real-time*
985 *photogrammetric monitoring*. 10724. https://doi.org/10.5194/egusphere-egu24-10724
986 Peltier, A., Bachèlery, P., & Staudacher, T. (2009). Magma transport and storage at Piton de La
987 Fournaise (La Réunion) between 1972 and 2007: A review of geophysical and geochemical
988 data. *Journal of Volcanology and Geothermal Research, Recent advances on the geodynamics*
989 *of Piton de la Fournaise volcano*, *184*(1), 93–108.
990 https://doi.org/10.1016/j.jvolgeores.2008.12.008
991 Peltier, A., Ferrazzini, V., Di Muro, A., Kowalski, P., Villeneuve, N., Richter, N., Chevrel, O., Froger,
992 J. L., Hrysiewicz, A., Gouhier, M., Coppola, D., Retailleau, L., Beauducel, F., Gurioli, L.,
993 Boissier, P., Brunet, C., Catherine, P., Fontaine, F., Lauret, F., … Ramsey, M. (2020).

994 Volcano Crisis Management at Piton de la Fournaise (La Réunion) during the COVID-19
995 Lockdown. *Seismological Research Letters*, *92*(1), 38–52.
996 https://doi.org/10.1785/0220200212
997 Peltier, A., Villeneuve, N., Ferrazzini, V., Testud, S., Hassen Ali, T., Boissier, P., & Catherine, P.
998 (2018). Changes in the Long-Term Geophysical Eruptive Precursors at Piton de la Fournaise:
999 Implications for the Response Management. *Frontiers in Earth Science*, *6*.
1000 https://doi.org/10.3389/feart.2018.00104
1001 Plank, S., Shevchenko, A. V., d'Angelo, P., Gstaiger, V., González, P. J., Cesca, S., Martinis, S., &
1002 Walter, T. R. (2023). Combining thermal, tri-stereo optical and bi-static InSAR satellite
1003 imagery for lava volume estimates: The 2021 Cumbre Vieja eruption, La Palma. *Scientific*
1004 *Reports*, *13*(1), 2057. https://doi.org/10.1038/s41598-023-29061-6
1005 Poland, M. P., Miklius, A., Jeff Sutton, A., & Thornber, C. R. (2012). A mantle-driven surge in
1006 magma supply to Kīlauea Volcano during 2003–2007. *Nature Geoscience*, *5*(4), 295–300.
1007 https://doi.org/10.1038/ngeo1426
1008 Poland, M. P., Miklius, A., & Montgomery-Brown, E. K. (2014). *Magma supply, storage, and*
1009 *transport at shield-stage Hawaiian volcanoes* (pp. 179–234). US Geological Survey.
1010 Pouclet, A., & Bram, K. (2021). Nyiragongo and Nyamuragira: A review of volcanic activity in the
1011 Kivu rift, western branch of the East African Rift System. *Bulletin of Volcanology*, *83*(2), 10.
1012 https://doi.org/10.1007/s00445-021-01435-6
1013 Quane, S. L., Garcia, M. O., Guillou, H., & Hulsebosch, T. P. (2000). Magmatic history of the East
1014 Rift Zone of Kilauea Volcano, Hawaii based on drill core from SOH 1. *Journal of*
1015 *Volcanology and Geothermal Research*, *102*(3), 319–338. https://doi.org/10.1016/S0377-
1016 0273(00)00194-3
1017 Reddin, E., Ebmeier, S., Bagnardi, M., Bell, A. F., & Bedón, P. E. (2024). Craters of habit: Patterns
1018 of deformation in the western Galápagos. *Volcanica*, *7*(1), Articolo 1.
1019 https://doi.org/10.30909/vol.07.01.181227

1020 Reynolds, R. W., Geist, D. J., & Kurz, M. D. (1995). Physical volcanology and structural
1021 development of Sierra Negra volcano, Isabela Island, Galápagos archipelago. *GSA Bulletin*,
1022 *107*(12), 1398–1410. https://doi.org/10.1130/0016-
1023 7606(1995)107%253C1398:PVASDO%253E2.3.CO;2
1024 Ripepe, M., Bonadonna, C., Folch, A., Delle Donne, D., Lacanna, G., Marchetti, E., & Höskuldsson,
1025 A. (2013). Ash-plume dynamics and eruption source parameters by infrasound and thermal
1026 imagery: The 2010 Eyjafjallajökull eruption. *Earth and Planetary Science Letters*, *366*, 112–
1027 121. https://doi.org/10.1016/j.epsl.2013.02.005
1028 Roult, G., Peltier, A., Taisne, B., Staudacher, T., Ferrazzini, V., & Di Muro, A. (2012). A new
1029 comprehensive classification of the Piton de la Fournaise activity spanning the 1985–2010
1030 period. Search and analysis of short-term precursors from a broad-band seismological station.
1031 *Journal of Volcanology and Geothermal Research*, *241–242*, 78–104.
1032 https://doi.org/10.1016/j.jvolgeores.2012.06.012
1033 Rowland, S. K. (1996). Slopes, lava flow volumes, and vent distributions on Volcán Fernandina,
1034 Galápagos Islands. *Journal of Geophysical Research: Solid Earth*, *101*(B12), 27657–27672.
1035 https://doi.org/10.1029/96JB02649
1036 Rowland, S. K., Harris, A. J. L., Wooster, M. J., Amelung, F., Garbeil, H., Wilson, L., & Mouginis-
1037 Mark, P. J. (2003). Volumetric characteristics of lava flows from interferometric radar and
1038 multispectral satellite data: The 1995 Fernandina and 1998 Cerro Azul eruptions in the
1039 western Galápagos. *Bulletin of Volcanology*, *65*(5), 311–330. https://doi.org/10.1007/s00445-
1040 002-0262-x
1041 Schipper, C. I., Jakobsson, S. P., White, J. D. L., Palin, J. M., & Bush-Marcinowski, T. (2015). The
1042 Surtsey Magma Series. *Scientific Reports*, *5*(1), 11498. https://doi.org/10.1038/srep11498
1043 Shevchenko, A. V., Dvigalo, V. N., Zorn, E. U., Vassileva, M. S., Massimetti, F., Walter, T. R.,
1044 Svirid, I. Y., Chirkov, S. A., Ozerov, A. Y., Tsvetkov, V. A., & Borisov, I. A. (2021).
1045 Constructive and Destructive Processes During the 2018–2019 Eruption Episode at Shiveluch

Volcano, Kamchatka, Studied From Satellite and Aerial Data. *Frontiers in Earth Science*, *9*. https://doi.org/10.3389/feart.2021.680051

Shreve, T., & Delgado, F. (2023). Trapdoor Fault Activation: A Step Toward Caldera Collapse at Sierra Negra, Galápagos, Ecuador. *Journal of Geophysical Research: Solid Earth*, *128*(5), e2023JB026437. https://doi.org/10.1029/2023JB026437

Singer, B. S., Jicha, B. R., Harper, M. A., Naranjo, J. A., Lara, L. E., & Moreno-Roa, H. (2008). Eruptive history, geochronology, and magmatic evolution of the Puyehue-Cordón Caulle volcanic complex, Chile. *GSA Bulletin*, *120*(5–6), 599–618. https://doi.org/10.1130/B26276.1

Singer, B. S., Thompson, R. A., Dungan, M. A., Feeley, T. C., Nelson, S. T., Pickens, J. C., Brown, L. L., Wulff, A. W., Davidson, J. P., & Metzger, J. (1997). Volcanism and erosion during the past 930 k.y. At the Tatara–San Pedro complex, Chilean Andes. *GSA Bulletin*, *109*(2), 127–142. https://doi.org/10.1130/0016-7606(1997)109%253C0127:VAEDTP%253E2.3.CO;2

Staudacher, T., Peltier, A., Ferrazzini, V., Di Muro, A., Boissier, P., Catherine, P., Kowalski, P., Lauret, F., & Lebreton, J. (2016). Fifteen Years of Intense Eruptive Activity (1998–2013) at Piton de la Fournaise Volcano: A Review. In P. Bachelery, J.-F. Lenat, A. Di Muro, & L. Michon (A c. Di), *Active Volcanoes of the Southwest Indian Ocean: Piton de la Fournaise and Karthala* (pp. 139–170). Springer. https://doi.org/10.1007/978-3-642-31395-0_9

Stearns, H. T., & Macdonald, G. A. (1946). *Geology and ground-water resources of the island of Hawaii* (Report No. 9; Bulletin). USGS Publications Warehouse. https://pubs.usgs.gov/publication/70160867

Sturkell, E., Einarsson, P., Sigmundsson, F., Hreinsdóttir, S., & Geirsson, H. (2003). Deformation of Grímsvötn volcano, Iceland: 1998 eruption and subsequent inflation. *Geophysical Research Letters*, *30*(4). https://doi.org/10.1029/2002GL016460

Sutton, A. J., Elias, T., & Kauahikaua, J. (2003). Lava-Effusion Rates for the Pu‘u ‘Õ‘ō-Kūpaianaha Eruption Derived from SO, Emissions and Very Low. *US Geological Survey professional paper*, *1676*, 137.

1072 Swanson, D. A. (1972). Magma Supply Rate at Kilauea Volcano, 1952-1971. *Science*, *175*(4018),
1073 169–170. https://doi.org/10.1126/science.175.4018.169
1074 Teasdale, R., Geist, D., Kurz, M., & Harpp, K. (2005). 1998 Eruption at Volcán Cerro Azul,
1075 Galápagos Islands: I. Syn-Eruptive Petrogenesis. *Bulletin of Volcanology*, *67*(2), 170–185.
1076 https://doi.org/10.1007/s00445-004-0371-9
1077 Thorarinsson, S., & Sigvaldason, G. E. (1962). The eruption in Askja, 1961; a preliminary report.
1078 *American Journal of Science*, *260*(9), 641–651. https://doi.org/10.2475/ajs.260.9.641
1079 Thordarson, T., & Larsen, G. (2007). Volcanism in Iceland in historical time: Volcano types, eruption
1080 styles and eruptive history. *Journal of Geodynamics, Hotspot Iceland*, *43*(1), 118–152.
1081 https://doi.org/10.1016/j.jog.2006.09.005
1082 Thordarson, T., & Sigmarsson, O. (2009). Effusive activity in the 1963–1967 Surtsey eruption,
1083 Iceland: Flow emplacement and growth of small lava shields. In T. Thordarson, S. Self, G.
1084 Larsen, S. K. Rowland, & Á. Höskuldsson (A c. Di), *Studies in Volcanology: The Legacy of*
1085 *George Walker* (Vol. 2, p. 0). Geological Society of London.
1086 https://doi.org/10.1144/IAVCEl002.4
1087 Tryggvason, E. (1984). Widening of the Krafla fissure swarm during the 1975–1981 volcano-tectonic
1088 episode. *Bulletin Volcanologique*, *47*(1), 47–69. https://doi.org/10.1007/BF01960540
1089 Tryggvason, E. (1986). Multiple magma reservoirs in a rift zone volcano: Ground deformation and
1090 magma transport during the September 1984 eruption of Krafla, Iceland. *Journal of*
1091 *Volcanology and Geothermal Research*, *28*(1), 1–44. https://doi.org/10.1016/0377-
1092 0273(86)90003-X
1093 Vasconez, F. J., Ramón, P., Hernandez, S., Hidalgo, S., Bernard, B., Ruiz, M., Alvarado, A., Femina,
1094 P. L., & Ruiz, G. (2018). The different characteristics of the recent eruptions of Fernandina
1095 and Sierra Negra volcanoes (Galápagos, Ecuador). *Volcanica*, *1*(2), Articolo 2.
1096 https://doi.org/10.30909/vol.01.02.127133

1097 Viccaro, M., Nicotra, E., Millar, I. L., & Cristofolini, R. (2011). The magma source at Mount Etna
1098 volcano: Perspectives from the Hf isotope composition of historic and recent lavas. *Chemical*
1099 *Geology*, *281*(3), 343–351. https://doi.org/10.1016/j.chemgeo.2010.12.020
1100 Vlastélic, I., Di Muro, A., Bachèlery, P., Gurioli, L., Auclair, D., & Gannoun, A. (2018). Control of
1101 source fertility on the eruptive activity of Piton de la Fournaise volcano, La Réunion. *Scientific*
1102 *Reports*, *8*(1), 14478. https://doi.org/10.1038/s41598-018-32809-0
1103 Wadge, G. (1980). Output rate of magma from active central volcanoes. *Nature*, *288*(5788), 253–
1104 255. https://doi.org/10.1038/288253a0
1105 Wadge, G. (1982). Steady state volcanism: Evidence from eruption histories of polygenetic
1106 volcanoes. *Journal of Geophysical Research: Solid Earth*, *87*(B5), 4035–4049.
1107 https://doi.org/10.1029/JB087iB05p04035
1108 Wadge, G., & Guest, J. E. (1981). Steady-state magma discharge at Etna 1971–81. *Nature*, *294*(5841),
1109 548–550. https://doi.org/10.1038/294548a0
1110 Walker, A. M. (1969). On the Asymptotic Behaviour of Posterior Distributions. *Journal of the Royal*
1111 *Statistical Society: Series B (Methodological)*, *31*(1), 80–88. https://doi.org/10.1111/j.2517-
1112 6161.1969.tb00767.x
1113 Wauthier, C., Cayol, V., Smets, B., D'Oreye, N., & Kervyn, F. (2015). Magma Pathways and Their
1114 Interactions Inferred from InSAR and Stress Modeling at Nyamulagira Volcano, D.R. Congo.
1115 *Remote Sensing*, *7*(11), Articolo 11. https://doi.org/10.3390/rs71115179
1116 White, S. M., Crisp, J. A., & Spera, F. J. (2006). Long-term volumetric eruption rates and magma
1117 budgets. *Geochemistry, Geophysics, Geosystems*, *7*(3).
1118 https://doi.org/10.1029/2005GC001002
1119 Williams Jr., R. S., & Moore, J. G. (1976). *Man against volcano: The eruption on Heimaey, Vestmann*
1120 *Islands, Iceland* (General Information Product, p. 20) [Report]. USGS Publications
1121 Warehouse. https://doi.org/10.3133/70039211

Wolfe, E. W., Garcia, M. O., Jackson, D. B., Koyanagi, R. Y., Neal, C. A., & Okamura, A. T. (1987). The Puu oo eruption of Kilauea volcano, episodes 1–20, January 3, 1983, to June 8, 1984. *US Geol Surv Prof Pap*, *1350*, 471–508.

Wright, T. L., & Klein, F. W. (2014). *Two hundred years of magma transport and storage at Kīlauea Volcano, Hawai'i, 1790-2008*. US Geological Survey.

Xu, W., Jónsson, S., Ruch, J., & Aoki, Y. (2016). The 2015 Wolf volcano (Galápagos) eruption studied using Sentinel-1 and ALOS-2 data. *Geophysical Research Letters*, *43*(18), 9573–9580. https://doi.org/10.1002/2016GL069820

Xu, W., Xie, L., Bürgmann, R., Liu, X., & Wang, J. (2023). The 2022 Eruption of Wolf Volcano, Galápagos: The Role of Caldera Ring-Faults During Magma Transfer From InSAR Deformation Data. *Geophysical Research Letters*, *50*(14), e2023GL103704. https://doi.org/10.1029/2023GL103704

Yamamoto, T., Kudo, T., & Isizuka, O. (2018). Temporal variations in volumetric magma eruption rates of Quaternary volcanoes in Japan. *Earth, Planets and Space*, *70*(1), 65. https://doi.org/10.1186/s40623-018-0849-x